AN ABSTRACT OF THE THESIS OF

James R. Silkey for the degree of Master of Science

in Chemistry presented on December 8, 1978

Title: Electrochemical Studies of Liquid Chlorocuprates(I)

Redacted for Privacy

Abstract approved: _____
John T. Yoke

This research emphasized fundamental physical and electrochemical studies of systems based on the room temperature fused salt, triethylammonium dichlorocuprate(I). Such systems, which must be maintained under a protective atmosphere, were also used in some preliminary battery studies.

Spectra of dark green solutions of copper (II) chloride in triethylammonium dichlorocuprate(I) obey Beer's law, with an absorption maximum at 402 nm, ε 2.02×10^3 lit/mol cm. This behavior is typical of chlorocuprate(II) complexes. No special behavior due to intervalence transfer absorption is observed.

Densities of solutions of various salts in triethylammonium dichlorocuprate(I) were determined dilatometrically in the range 25-50°C, permitting concentrations to be expressed both on weight and molarity bases. The endothermic formation of liquid triethylammonium dichlorocuprate(I) involved a 10.9% increase in molar volume.

The specific conductance of triethylammonium dichlorocuprate(I) increases from 4.3×10^{-3} to 1.2×10^{-2} ohm^{-1} cm^{-1} in the range 25 to 50°C. Solutions of copper(I), copper(II), lithium, and triethylammonium chlorides in triethylammonium dichlorocuprate(I) all have lower

conductances than the neat solvent. The viscosities of solutions of copper(I) and copper(II) chlorides in triethylammonium dichlorocuprate(I) were determined in the range 25-50°C and found to be greater than that of the neat solvent. The temperature variations of the conductance and of the viscosity were both found to show Arrhenius-type behavior. Activation energies for viscous flow were in the typical range for fused salts, but activation energies for conductance were about three times larger than usual. A relation proposed by Frenkel, $\eta\kappa^{(E_\eta/E_\Lambda)}$ = constant, was closely followed by the mixtures.

The $Cu/Et_3NHCuCl_2$ electrode was a satisfactory reference electrode for potentiometric measurements in the fused salt systems. Its operational potential was -.24 volt vs. SCE at 25°. In polarization studies the time required to regain equilibrium following the passage of various currents was measured.

Potentiometric measurements were made of the cells $Cu/Et_3NHCuCl_2/Et_3NHCuCl_2$, $CuCl_2$ (M)/Noble Metal. In addition to a platinum electrode, a special Optically Transparent Thin Layer Electrode (OTTLE) was used, made of gold minigrid having 82% optical transparency. Approximate Nernstian behavior was observed only at low copper(II) concentrations.

Combined spectrophotometric and coulometric measurements of electrolysis in the OTTLE cell $Cu/Et_3NHCuCl_2/Au$ confirmed copper(II) chloride and copper as the oxidation-reduction products. The relation of faradays to moles of copper(II) was not accurate due to non-uniformity of the latter on the minigrid.

Bipolar voltage sweep studies were carried out in triethylammonium dichlorocuprate(I) cells with a platinum or glassy carbon working

electrode, a platinum auxiliary electrode, and the copper reference electrode. Shapes of the cyclic voltammograms showed great temperature dependence in the range 13-51°C. Peak potentials and currents showed linear dependence on the square root of the scan rate. Such behavior indicates blockage of the electrode surface by a poorly conducting film of electrolysis product. A viscous film of copper(II) chloride could be observed visually.

The Butler-Volmer equation was applied to overpotential-current relations in both high and low overpotential regions of the $Cu/Et_3NHCuCl_2$ and the $Pt/Et_3NHCuCl_2$, $CuCl_2(M)$ half-cells. Linearity of current-overpotential plots in the 5 mv > η > -5 mv region indicates that each of these half-cells is reversible. Tafel slopes were constructed to current-overpotential curves in the range 500 mv > η > -500 mv, from which values of the transfer coefficient were calculated.

Preliminary design and testing of batteries was undertaken. These batteries employed copper and flexible graphite or platinum foil electrodes, with various separators. Some were prepared in a charged condition with a solution of copper(II) chloride in triethylammonium dichlorocuprate(I) in contact with the inert electrode. Some were prepared using only triethylammonium dichlorocuprate(I) and were charged by passage of current from an external source. Measurements of open circuit voltages and of potential-current-time discharges were made. The major practical problem with these cells was their high internal resistance.

Electrochemical Studies of Liquid Chlorocuprates(I)

by

James R. Silkey

A THESIS

submitted to

Oregon State University

in partial fulfillment of
the requirements for the
degree of

Master of Science

Completed December 8, 1978

Commencement June 1979

APPROVED:

Redacted for Privacy

Professor of Chemistry in charge of major

Redacted for Privacy

Chairman of Department of Chemistry

Redacted for Privacy

Dean of Graduate School

Date thesis is presented December 8, 1978

Typed by Kathryn Miller for James R. Silkey

ACKNOWLEDGMENTS

I wish to express appreciation to Dr. John T. Yoke for his support and expert guidance in this research. Also, thanks to Dr. Harry Freund for helpful discussions and suggestions.

I wish to thank Virgil G. Hiatt and Dr. H. Michael Wehr, of the Oregon State Department of Agriculture, for their assistance in obtaining partial financial support from the Oregon State Department of Agriculture, and allowing the time to be taken for this work.

Acknowledgment is made to the Oregon State University Research Council for funds used in the construction of the optically transparent thin layer electrochemical cell and other apparatus.

I wish to express appreciation to my wife Vicki, for her patience and encouragement during the course of this study. Her help in typing the rough draft of this dissertation is also gratefully acknowledged.

TABLE OF CONTENTS

TABLE OF CONTENTS (Cont.)

LIST OF FIGURES

LIST OF FIGURES (Cont.)

LIST OF FIGURES (Cont.)

LIST OF TABLES

Electrochemical Studies of Liquid Chlorocuprates

I. INTRODUCTION

The discovery of room temperature fused salt mixtures (1) of the type copper(I) chloride-triethylammonium chloride has provided a convenient medium for studying the behavior of molten electrolytes. Recent investigations of these liquid electrolytes have focused on the spectroscopic characterization (2) of solute species and on measurement of certain electrochemical properties (3). The high concentrations of ions present in these low melting systems has also suggested their application in electrical energy storage systems, with potential thermal energy and corrosion advantages over the more familiar high temperature fused salt electrolyte media. The present research represents an effort to provide a better understanding of certain electrochemical and physical properties of triethylammonium dichlorocuprate(I), and to conduct some preliminary cell design studies.

The investigation of high temperature fused salt galvanic cells had been motivated by anticipation of higher theoretical energy storage densities in those systems than are obtainable in conventional batteries. Room temperature fused salts offer distinct advantages over their high temperature counterparts, namely, operation under ambient conditions and ease of handling during use. In the final analysis, however, it is actual cell performance in areas such as current and voltage output, amp-hour capacity and energy density which will be of practical importance. This information must be obtained from the study of prototype cells.

Prior to engineering any battery, fundamental electrochemical measurements such as of conductivities, exchange currents and potentials should be obtained. Attention should be paid to interrelationships of all cell components. These investigations will provide an opportunity for comparison of properties of the room temperature fused salt mixture with those of the more convential high temperature fused salts.

In addition to fundamental physical and electrochemical studies, preliminary attempts to design and evaluate cells based on room temperature fused salt mixtures were of interest in this research.

II. HISTORICAL

Room Temperature Fused Salts - A Survey of Previous Work

Most simple inorganic salts melt well above room temperature. There is a great deal of interest in these high temperature liquids as solvents and media for chemical and especially electrochemical processes, as well as interest in them for their own sake in fundamental studies of the liquid state (4). Such typical molten salts have three obvious disadvantages in practical application: they are corrosive, energy is consumed in achieving and maintaining the high temperature, and thermally sensitive solutes cannot be used.

The applications of fused salts in organic chemistry have been reviewed (5). Salts derived from organic amines are of particular interest; for example, a number of quaternary ammonium halides have melting points of 100°C or less. Salts with organic ammonium cations and complex inorganic anions may have much lower melting points. For example, the phase diagram of the N-ethylpyridinium bromide-aluminum chloride system shows a melting temperature of 45°C at the 1:1 composition N-Etpy$^+$AlCl$_3$Br$^-$ and of -40°C at the 1:2 composition N-Etpy$^+$Al$_2$Cl$_6$Br$^-$. Such low melting combinations of quaternary ammonium halides and various metal halides have been used as media for the cathodic electrodeposition of the metals (6), and for various catalytic reactions of olefins (7).

A plan to synthesize tetraalkylammonium tetraalkylboride salts which would have low lattice energies for steric reasons succeeded in giving a number of compounds, such as $[(C_2H_5)_3(C_6H_{13})N]^+$ $[B(C_2H_5)_3(C_8H_{17})]^-$, which are liquids at room temperature and form

glasses on cooling to -78°C (8).

Various solid salts containing organic ammonium cations and chlorocuprate(I) anions have long been known. Remy and Laves (9) prepared solids of the compositions $[CH_3NH_3][CuCl_2]$, $[CH_3NH_3]_2[CuCl_3]$, $[(CH_3)_2NH_2][Cu_2Cl_3]$, $[(CH_3)_2NH_2][CuCl_2]$, $[(CH_3)_3NH][Cu_2Cl_3]$, $[(CH_3)_3NH]_2[CuCl_3]$, $[(CH_3)_4N][Cu_2Cl_3]$, and $[(CH_3)_4N]_2[CuCl_3]$. With ethyl-substituted ammonium salts, previous work in this laboratory has led to the preparation of the solids $[C_2H_5NH_3][CuCl_2]$, $[(C_2H_5)_2NH_2][CuCl_2]$, and $[(C_2H_5)_4N][CuCl_2]$ (2, 10, 11). Solid chlorocuprates(I) with many other cations have been prepared.

Following the discovery by J. F. Weiss et al. at the University of Arizona, of the liquid nature of triethylammonium dichlorocuprate(I) at room temperature, several other room temperature liquids containing equimolar amounts of trialkylammonium chlorides or triethylphosphonium chloride and copper(I) chloride were prepared (2) at Oregon State University and at Hampden-Sydney College. The work on triethylphosphonium and triethylchlorophosphonium dichlorocuprate(I) was part of the doctoral research of D. D. Axtell at Oregon State University. The further work on the organic ammonium salts was a project of Professor William Porterfield during a summer spent at Oregon State University, and was continued by him and by his students at Hampden-Sydney College. In all cases the trialkyl substitution with ethyl or larger groups seemed to be necessary for the liquid to form at room temperature. This suggested a cationic steric effect on the lattic energy to be at least partially responsible for the low melting points.

Vibrational frequencies attributed to $CuCl_2^-$ and $Cu_2Cl_3^{2-}$ were

identified in the Raman spectra of the liquid triethylammonium dichlorocuprate(I), and of triethylammonium dichlorocuprate(I) in which extra copper(I) chloride or triethylammonium chloride had been dissolved. Complex anion equilibria, which have been observed in chloride-enriched aqueous solutions of copper(I) chloride (12) and may be postulated to exist in triethylammonium dichlorocuprate(I) are

$$CuCl_2^- + Cl^- \rightleftarrows CuCl_3^{2-}$$

$$CuCl_2^- + CuCl \rightleftarrows Cu_2Cl_3^-$$

The presence of several of these complex species would contribute to the melting point depression of the mixture and this is thought to be a second factor in the stabilization of the liquid state.

Triethylammonium dichlorocuprate(I) is a viscous oil with a reported specific conductance of 3.84×10^{-3} $ohm^{-1}cm^{-1}$ at 25°C (3). The compound remains liquid to below 0°C and upon further cooling forms a glass. Temperatures in excess of 110°C cause the loss of triethylamine. The pure fused salt has a yellow color resulting from the tail of an ultraviolet charge transfer band which extends into the visible region (13). Triethylammonium dichlorocuprate(I) and its mixtures must be protected from air since they will absorb oxygen and darken quickly if contaminated.

In work at Hampden-Sydney College, the technique of cyclic voltammetry was employed in additional studies of triethylammonium dichlorocuprate(I) (3). Cyclic voltammetry of an acetonitrile solution of the salt (0.042 M) showed the existence of several electroactive species. Some of these electrochemical reactions appeared to be irreversible in acetonitrile solution although the reproducibility of

the number of peaks was affected by electrolyte age.

Attempts were made to prepare a cell with two platinum electrodes and using triethylammonium dichlorocuprate(I) as both anolyte and catholyte. On partial charging, this cell developed a voltage of 0.85 v (3). Difficulties observed with this cell included electrolyte gelling at elevated copper(II) concentrations, formation of dendritic copper growths during charging, low current output and rapid voltage drop on partial discharge.

Spectra and Structure of Complex Chlorocuprates(I) and (II)

Since the electrochemical processes being considered in this work involve mixtures of copper(II) chloride or of chlorocuprate(II) complexes with the triethylammonium dichlorocuprate(I) fused salt, which may have various chlorocuprate(I) complexes present in it, it is of interest to consider the spectroscopic properties of the copper(I) and copper(II) complexes when separate and when mixed together. Spectrophotometric studies might provide an experimental approach to the systems of interest which would complement electrochemical measurements.

The pale yellow color of neat triethylammonium dichlorocuprate(I) (which becomes progressively more green if the fused salt becomes partly oxidized by traces of oxygen) is due to the tail of an intense ultraviolet absorption. Porterfield (3) found the neat liquid to have a UV cutoff below about 26,000 cm^{-1} (385 nm) but to be transparent in the visible region. He showed that the room temperature fused salt could be used as a chloride ion-rich solvent, analogous to the molten alkali chloride eutectics, to obtain visible region spectra of various

chloro-complexes of the transition metals.

It has long been known that insoluble copper(I) chloride dissolves in concentrated aqueous chloride ion solutions to give a variety of chlorocuprate(I) complexes. These exhibit several absorption maxima in the ultraviolet region. Russian workers (13) have attributed peaks at 273 nm and in the 300-400 nm range to the $CuCl_3^{2-}$ ion and to polymeric species of the type $[Cu_nCl_{n+1}]^-$, respectively. Such species, $CuCl_3^{2-}$ and $Cu_2Cl_3^-$, were identified by Axtell and co-workers (2) in neat triethylammonium dichlorocuprate(I) (and in the fused salt containing extra copper(I) or triethylammonium chloride dissolved in it) by Raman spectroscopy.

The structural chemistry and related spectral properties of copper(II) in its compounds and complexes exhibit enormous variety. Copper(II) is well-known in six-, five-, and four-coordinate environments. According to a simple ligand field model of d^9 copper(II) in octahedral coordination, a single electronic transition would be expected, typically in the near-infrared region at about 1000 nm. While some copper(II) compounds, such as the anhydrous sulfate, are in fact colorless, the vast majority absorb in the visible region and are colored. One source of transitions in the visible region for copper(II) species in general is ligand to metal charge transfer. Another source, for six-coordinate copper, is the splitting by the Jahn-Teller distortion of the single ligand field transition into a number of components.

For example, the Jahn-Teller effect causes the hexaaquocopper(II) ion to have four close water ligands and two more distant water ligands in the <u>trans</u> positions of a distorted octahedron. The near-infrared

absorption peak is very broad and tails into the high wavelength end of the visible region, giving rise to the pale blue color. As water ligands are replaced by ligands of higher field strength, such as ammonia, the whole band is slightly shifted to higher energy. This shift has a very large effect on the integrated intensity of the tail in the visible region, with a marked deepening of the blue color. On the other hand, replacement by ligands of weaker field strength, such as chloride ions, causes the peak to move to lower energy, more into the near-infrared region.

Blue-green hydrated copper(II) chloride takes on a drab brown color on dehydration. The structure of anhydrous copper(II) chloride (14) is based on linked polymer chains, with four Cl^- in a square plane at 2.30 Å and two <u>trans</u>- Cl^- at 2.95 Å giving a distorted octahedron about each copper. The reflectance spectrum of the powder has been obtained by Clifton (15) in the 400-960 nm region; he found a maximum at 800 nm. Hatfield and Piper (16) reported it at 820 nm. The absorption of anhydrous copper(II) chloride across the entire visible region is due to the overlap of tails of this near-infrared peak and of the intense charge transfer absorptions in the ultraviolet region. The various chlorocuprate(II) complexes, which may be yellow, brown, orange, or green, all have a charge transfer band in about the same region, at 370 nm for the trigonal bipyramidal $CuCl_5^{3-}$, 402 nm for square planar $CuCl_4^{2-}$, 417 nm for distorted tetrahedral $CuCl_4^{2-}$, 407 nm for the distorted octahedral species in solid $CsCuCl_3$, and 385 nm for aqueous copper(II) in concentrated chloride ion solutions.

When a metal is present in two oxidation states simultaneously,

there may be special spectral features not seen for either oxidation state individually. Such "Intervalence Transfer Absorption" has been reviewed by Allen and Hush (17, 18), who classify mixed copper(I)-copper(II) systems under the category "Symmetrical Homonuclear Intervalence Transfer Outer Sphere Complexes", although the simplest example they give is of a chloro-bridged inner sphere complex,

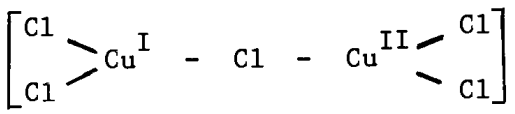

This species was postulated by McConnell and Davidson (19) as the chromophore responsible for the extra intensity of absorption in the 400-500 nm region of solutions of copper(I) chloride in concentrated hydrochloric acid - copper(II) chloride mixtures. Such absorption, above that observed when the colorless copper(I) chloride was absent, did not occur, however, in the form of an absorption peak or maximum in the wavelength region studied.

Mori and Fujiwara (20) prepared a number of compounds containing hexaammine complex cations of Cr, Co, and Rh(III) with chlorocuprate anions. In different cases, the latter contained all Cu(I), or all Cu(II), or mixtures of Cu(I) and Cu(II). Culpin and co-workers (21) found that both the all Cu(I) salt $[Co(NH_3)_6]_4Cu_5Cl_{17}$ and the all Cu(II) salt $[Co(NH_3)_6]CuCl_5$ have the orange-yellow color of the hexaammine cobalt(III) cation, with no absorptions in the visible region due to the chlorocuprate complexes. The mixed Cu(I) - Cu(II) species possess a new band, at 588 nm, whose intensity passes through a maximum at a Cu(I)/Cu(II) ratio of 1:1 and which causes the materials to have an orange-brown to black color. Hush (18) locates this new mixed

chlorocuprate band at 595 nm when the cation is the Co(III) complex, at 615 nm with the Cr(III) complex, and at 550 nm with the Rh(III) complex. The spectral effect in these salts cannot be due to an inner-sphere chloro-bridged complex of the type postulated by McConnell and Davidson, since a crystallographic study showed the $[M(NH_3)_6]^{3+}$ salts to contain Cu(I) tetrahedrally coordinated by Cl^- and Cu(II) in trigonal bipyramidal coordination by Cl^-.

Another report seems inconsistent with the wavelengths of the new mixed valence absorption peak and the resulting color effects noted above. Mori and Fujiwara also prepared a yellow $CuCl_5^{3-}$ chlorocuprate(II) compound containing the colorless organic cation $H_2N(CH_2CH_2NH_3)_2^{3+}$. This could be doped with a little copper(I), which caused the color to become very dark green. Hush then reported the Cu(I) - Cu(II) absorption peak in this green material to be at 550 nm. Dissolution of white copper(I) chloride in a green aqueous copper(II) chloride-concentrated hydrochloric acid solution causes the mixture to become a dark olive green to black color. Exposure to air of triethylammonium dichlorocuprate(I), which leads to some oxidation to copper(II) causes the color to become dark green to black. It seems unlikely that the intervalence absorption of these dark green materials would be in the same wavelength region as for the orange-brown materials described above.

Conductivity and Viscosity

The equivalent conductance ($ohm^{-1}cm^2equiv^{-1}$) of a fused salt is calculated from the specific conductance, κ, ($ohm^{-1}cm^{-1}$) by application of the equation $\Lambda = \frac{\kappa E}{\rho}$, where E is the equavalent weight and ρ is the

density of the molten salt (22). For mixtures of salts, the equivalent weight, $\bar{E}$, is calculated from $\bar{E} = \Sigma f_i E_i$, where E_i is the equivalent weight and f_i is the fraction of the total equivalents contributed by the ith component. The number of equivalents of any component is equal to the product of its concentration and the charge on the cation, $C_i Z_i$. The equivalent fraction then is $C_i Z_i / \Sigma C_i Z_i$.

The effects of temperature on conductivity of molten salts have been shown theoretically (23) and experimentally (24) to follow equations of the type $\Lambda = A \exp(-E_\Lambda/RT)$ and $\kappa = A \exp(-E_\kappa/RT)$. Changes in the conductances of binary mixtures of fused salts are similarly described, but by more complex equations of the type $\Lambda = A_1 \exp(-E_1/RT) + A_2 \exp(-E_2/RT)$, where E_1 and E_2 represent activation energies of the principle charge carriers (25). Careful studies of the conductances of alkali chlorides have shown that the relation $\Lambda = A \exp(-E_\Lambda/RT)$ is not exactly followed and that log Λ - 1/T plots are slightly curved for all alkali chlorides except lithium chloride. These equations are not applicable to incompletely dissociated salts or to compounds which may exhibit changes in ionic concentration or transference numbers with temperature (26). Activation energies for conductance in fused alkali halides fall in the range 1-4 kcal/mole.

A similar relation, $\eta = A \exp(-E_\eta/RT)$, has been successfully used to describe the temperature dependence of the viscosity of concentrated aqueous electrolytes, fused salts, and fused salt mixtures (27, 28, 29, 30). Activation energies for viscous flow in fused salts are usually found to be in the range 3-11 kcal/mole.

For molten salts the ratio of activation energies, E_η/E_Λ, has been

found experimentally to vary between 3 and 7 for univalent chlorides and between 2 and 7 for bivalent chlorides (30). Thus, the activation energy barriers involved in ionic migration are less than those encountered in viscous flow.

While Walden's rule, $\eta\Lambda$ = const., is generally not followed for most fused salts (31) when temperature induced variations in viscosity are encountered, the empirical relationship of Frenkel (32), $\eta\kappa^{(E_\eta/E_\Lambda)}$ = const., has been experimentally verified (30, 33). Although there appears to be little significance to Frenkel's equation, its apparent validity suggests the mutual relationship of conductance and viscous flow mechanisms to the same fundamental properties of the constituents of the melt (33).

Potentiometry

The reversibility of electrochemical reactions can be defined using either a chemical or thermodynamic basis (34). Thermodynamic reversibility requires an infinitely fast (35) oxidation-reduction reaction to maintain equilibrium conditions at the electrode where a net current flows. This type of operation does not exist in practice, so while a finite, but very small, displacement from the electrode equilibrium potential may occur this is still generally termed reversible operation. Indeed, all that is required is for the oxidation-reduction reaction to proceed rapidly enough to maintain nearly the original equilibrium electrode reaction rates under the experimental conditions (36). Potentiometric measurements of galvanic cell potentials, obtained under equilibrium conditions, can provide a means for estimating the

thermodynamic reversibility of a particular electrode reaction by allowing comparison of the cell EMF data with that predicted for a Nernstian electrode. This approach requires liquid junction potentials to be small or nearly constant for all cells studied.

The chemical reversibility of a particular electrode reaction can also be determined from overpotential-current measurements in the voltage range near the equilibrium potential and from polarization-time curves (37, 38, 39). Hysteresis of the anodic and cathodic overpotential curves, obtained within several millivolts of the equilibrium electrode potential, indicates irreversible behavior while linearity of both branches suggests a more reversible reaction. The magnitude of electrode polarization during passage of a constant current also helps in assessing reversible behavior.

Electrode potentials in triethylammonium dichlorocuprate(I) as a function of electrolyte composition have not been studied previously. However, a galvanic cell of the type

$$Pt/Et_3NHCuCl_2/Et_3NHCuCl_2/Pt$$

was prepared and charged to give an open circuit voltage of 0.85 v at 1% of maximum theoretical charge (3). This voltage decreased after charging was stopped, presumably as a result of diffusion of copper(II) chloride formed at the anode into the bulk electrolyte.

Fundamental potentiometric studies of a cell in which the electrode reactions are

$$Cu + 2Cl^- \rightleftarrows CuCl_2^- + e^-$$

and $$CuCl_2 + e^- \rightleftarrows CuCl_2^-$$

in triethylammonium dichlorocuprate(I) as solvent require measurements

using half-cells of the type $Cu/Et_3NHCuCl_2$(liq.) and Noble Metal/ $Et_3NHCuCl_2$(liq.), $CuCl_2$(M). For this purpose, establishment of a relative reference electrode potential is essential, and establishment of its relation to the thermodynamic scale is desirable. Such a reference electrode should not be polarized under experimental conditions and should provide a stable reproducible potential. In addition, both the electrode and its potential-determining ions in solution should be inert towards the solvent and other electrode. If this last requirement cannot be satisfied, the reference half cell must be separated from the working solution with a salt bridge. However, the anhydrous nature of room temperature fused salts precludes the use of aqueous salt bridges over extended periods of time.

Overpotential Studies

The relationship between electrode current and the magnitude of electrode polarization, the overpotential, is fundamentally important to the understanding of electrode-electrolyte interactions. Important quantities derivable from these data include exchange current densities, electrochemical reaction orders, stiochiometric numbers and the symmetry factor or in the case of complex reactions (40), charge transfer coefficients.

The basic equation relating current and charge transfer overpotential is the Butler-Volmer equation which, in the form of equation (1), is applicable to simple as well as to complex multistep electrochemical reactions (41).

$$i = i_o\left\{ \exp\left[\left(\frac{n-\vec{\gamma}}{\nu}\right) - r\beta\right)\frac{F\eta}{RT}\right] - \exp\left[-\left(\frac{\vec{\gamma}}{\nu} + r\beta\right)\frac{F\eta}{RT}\right]\right\} \qquad (1)$$

Variables in this equation are the number of electrons involved in the overall reaction, n, the number of electrons transferred before the rate determining step, $\vec{\gamma}$; the number of times the rate determining step must occur for the stoichiometric reaction to occur once, ν; the symmetry factor, β; the overpotential, η; and r which assumes values of 1 or 0 for charge transfer or chemical rate determining steps respectively. For an uncomplicated one electron reaction where the charge transfer reaction is rate determining, the following simplified expression results.

$$i = i_o \{\exp [(1-\beta)\eta F/RT] - \exp(-\beta\eta F/RT\} \qquad (2)$$

However, in the case of complex multistep reaction mechanisms, α_{anodic} and $\alpha_{cathodic}$ are substituted for the quantities $(1-\beta)$ and (β), respectively, in equation (2). The resulting equation is then equivalent to equation (1), in which $(\frac{n-\vec{\gamma}}{\nu} - r\beta)$ and $(\frac{\vec{\gamma}}{\nu} + r\beta)$ are reduced to α_{anodic} and $\alpha_{cathodic}$ respectively. Thus, the high and low overpotential approximations to the Butler-Volmer equation are valid for complex as well as simple reaction mechanisms:

Low overpotential approximation: $i = i_o(\frac{nF\eta}{\nu RT})$

High overpotential approximation:

$$i_{anodic} = i_o \exp(1-\beta)F\eta/RT$$

$$\text{or } i_{anodic} = i_o \exp(\alpha_{anodic}F\eta/RT)$$

and $$i_{cathodic} = i_o \exp(-\beta F\eta/RT)$$

$$\text{or } i_{cathodic} = i_o \exp(-\alpha_{cathodic}F\eta/RT)$$

In the low overpotential approximation, the stoichiometric number, ν, and the exchange current, i_o, are both variables in the case of a complex reaction ($\nu > 1$) and one must be known or assumed in order for the

expression to be useful.

In electrochemical reactions involving only one electron, where charge transfer is rate determining, the anodic and cathodic branches of the η vs. $\log|i|$ curves have characteristic shapes (41, 42). Under these conditions symmetrical anodic and cathodic branches of the η vs. $\log|i|$ curves indicate $\beta = 0.5$.

In addition to charge transfer, other sources of overpotential or polarization can affect the shape of η vs. $\log|i|$ curves. Other causes of polarization may be separated into reaction, diffusion, crystallization and ohmic overpotentials (43). Concentration overvoltage is considered to result from effects of both reaction and diffusion overvoltages. Pure concentration overvoltage may be differentiated from pure reaction overvoltage by realizing that only a diffusion limited current will increase with stirring. The presence of charge transfer overpotential is confirmed by the existence of a linear Tafel slope in the η vs. $\log|i|$ plot, at potentials where concentration overpotential would be negligible. Crystallization overpotential cannot be determined by direct current methods because of surface changes during electrode polarization.

The total overpotential for a reaction is the sum of all previously mentioned overpotentials. The effect of each overpotential, then, is to decrease the electrode current observed at a given potential.

Voltammetric Effects of Anodic Film Formation

General effects associated with electrode surface coverage by anodic reaction products have been summarized by Erdey-Gruz (44) and

Bockris (45). Explanations of these processes involve the precipitation of initially soluble anodic products and the formation of poorly conducting porous and non-porous crystalline surface layers. General theories of film formation and their predicted current-time relationships have been developed (44, 46).

During the progress of an anodic reaction, where film formation at the electrode surface occurs, the normal current-voltage relationships predicted from mass transfer effects and concentration changes are altered, and a considerable decrease in the rate of the reaction is observed. Relationships developed for film formation during anodic metal dissolution can be applied to anodic reactions where the electroactive material must diffuse to the electrode from the bulk solution. Experimental observations of anodically produced copper(I) chloride films on a copper electrode and of parathiocyanogen, $(SCN)_x$, film formation on a platinum electrode follow the same mathematical model (46). Current-voltage curves for these systems were found to be very similar to Figure 1.

Muller's model for passivity (47) was used to develop the current-voltage relationship where anodic formation of a poorly conducting film occurs (46). Charging of a cell containing the triethylammonium dichlorocuprate(I) electrolyte would give copper(II) chloride as the anodic product and this has been shown to be a poorly conducting material (48). According to Muller, film formation commences from a number of sites and spreads over the electrode surface leaving a porous coating. Initially the thickness of the passivating layer is constant, but once the surface is effectively covered the depth of the film increases while

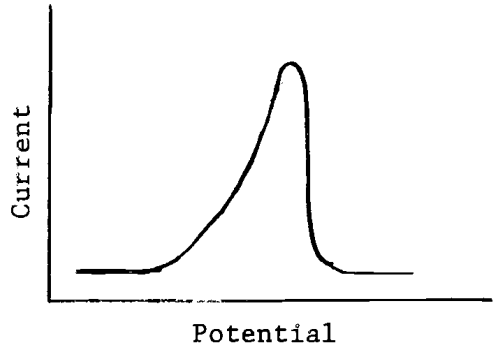

Figure 1. Current-voltage curve predicted for an electrode where resistive film formation occurs.

maintaining constant pore area. Concentration polarization and mass transfer of anodic products are assumed negligable. Theoretical equations (46) predict the peak current and potential of Figure 1 to increase linearly with the square root of the voltage scan rate provided the surface coverage is independent of the scan rate.

Primary Battery Fundamentals

While strictly speaking a battery is an assembly of two or more cells, the common usage in the trade of referring to a single cell as a battery will be followed in this thesis. The development of all modern electrochemical energy storage cells of practical importance have necessarily been the result of extensive developmental programs. Modern electrochemical theories and techniques are beginning to change the manner in which research is carried out (49). However, the classical Edisonian, or intuitive approach to development is difficult to abandon completely, especially during a short term project.

Before embarking on a program consisting of making and testing one battery after another to determine the effects of varying experimental

conditions on battery performance, it is best to determine some of the fundamental properties of the system to be developed. Basic properties of battery components which are important in obtaining high voltage and current outputs are the electrode exchange current, limiting current (mass transport related), and electrolyte resistance (50). These three quantities are related to other properties of the system such as the physical state and area of the electrodes, reversibility at the electrode, electrode-electrolyte geometry and electrolyte composition and viscosity. All of these characteristics should be studied.

A battery is generally composed of a casing, anode and anolyte, cathode and catholyte, and separator. The electrode characteristics can be studied using standard overpotential and conductance techniques. Altering the composition of the electrolyte can be used to lower the internal cell resistance. This resistance is related to the electrolyte and separator conductivities. The separator functions as a barrier to prevent internal chemical short circuiting in the charged battery, but it must also maintain a low resistance. These functions require a delicate balance and the choice of separator will depend on electrolyte composition.

After sufficient information has been obtained to justify a particular battery configuration, two output characteristics of the final cell should be measured. These are the open circuit voltage and voltage-time discharge curves. These data will allow calculation of the percent of theoretical discharge, power output and practical energy storage density. Since the energy storage density will vary with the rate of discharge, it may be of interest to determine the magnitude of this dependence.

III. EXPERIMENTAL

Materials

Reagents

Copper(II) chloride. ACS Reagent Grade copper(II) chloride dihydrate (J. T. Baker or Mallinckrodt) was used without further purification. Anhydrous copper(II) chloride was prepared by heating the dihydrate at 110°C for 18 hours.

Lithium chloride. Reagent Grade lithium chloride was dehydrated at 110°C for 18 hours. The anhydrous salt was both ground and stored in the dry box.

Copper(I) chloride. Copper(I) chloride was prepared by the sulfite reduction method of Keller and Wycoff (51). The product was washed successively with glacial acetic acid, absolute ethanol and peroxide-free ether. After drying, the product was stored in the dry box.

Ethyl ether was freed from peroxides by shaking with ca. 10% aqueous ferrous ammonium sulfate. The ether layer was dried over sodium sulfate and distilled from sulfuric acid.

Triethylamine. Practical grade triethylamine was distilled and the 87-89° fraction retained.

Triethylammonium chloride. Triethylammonium chloride was prepared by reaction of triethylamine with 6 M hydrochloric acid. Excess water was evaporated and the white solid was purified by three successive recrystallizations from absolute ethanol. The product was oven dried, ground and reheated to 110°C for 18 hours prior to storage in the dry box.

Grafoil. Grafoil, a flexible, conductive graphite sheeting is a registered trademark of the Union Carbide Company. A Grafoil sample was kindly supplied by Dr. D. D. Schmidt of the Dow Chemical Company, who reports that it is prepared by treating graphite flake with a nitric acid-sulfuric acid mixture, rapidly heating the treated graphite to 1000° , and compressing.

Copper foil. Five mil J. T. Baker 100% copper sheet was used.

Potassium ferricyanide. Mallinckrodt ACS Reagent Grade potassium ferricyanide was used without further purification. Anal. Calcd. for $K_3Fe(CN)_6$: Fe, 16.96%. Found: Fe, 16.88%.

Glycerol. J. T. Baker Reagent Grade glycerol, 95.1%, was used without further purification.

Methylcellulose. A one percent aqueous solution of Dow Methocel 60 HG was prepared by dissolving two grams in 200 ml of boiling distilled water.

Solvents

Acetonitrile. Acetonitrile (Matheson Coleman and Bell) was dehydrated by shaking with phosphorus pentoxide. The solvent was subsequently distilled from phosphorus pentoxide and stored in the dry box.

Inert Atmosphere Techniques in Preparation and Handling of Triethylammonium Dichlorocuprate(I) and Fused Salt Mixtures

Triethylammonium dichlorocuprate(I), as a neat oil, was prepared by mixing equimolar quantities of powdered triethylammonium chloride and copper(I) chloride. Fused salt mixtures of triethylammonium

dichlorocuprate(I) containing lithium chloride, copper(II) chloride, or additional triethylammonium chloride or copper(I) chloride were prepared by dissolving the solid in neat triethylammonium dichlorocuprate(I). All fused salt mixtures were prepared and transferred under Pre-purified Grade nitrogen in a Forma stainless steel dry box. Entrance to the box was through an evacuable port. The unit was fitted with a gas purification system, through which the box atmosphere was continuously circulated, consisting of a tower containing supported BTS catalytic activated copper oxygen remover and tubes containing Linde 4A, 5A, and 13X molecular seives.

Cells for dilatometric, viscosimetric, spectrophotometric, conducimetric, and various electrochemical measurements, as well as all test batteries, were loaded with the appropriate fused salt mixtures under nitrogen in the dry box, and sealed with standard taper stoppers, black wax such as Fisher Scientific Company Pyseal, stopcock grease, etc. as appropriate.

Instrumentation

Electrochemical Polarization and Coulometric Studies

Electrochemical polarization and coulometry studies were carried out with a Princeton Applied Research Model 173 potentiostat/galvanostat fitted with a Model 179 digital coulometer. Current and potential data were either recorded on a Heath Model SR 204 recorder or read directly from a Fairchild Model 7030 digital voltmeter.

Voltage Sweep Experiments

Potential-current relationships for several electrode materials in contact with fused salt mixtures were investigated using a Princeton Applied Research Model 174 polarograph. Current-voltage curves for the slow voltage sweep experiments were recorded with a Varian F80A X-Y recorder.

Potential Measurements

EMF measurements of fused salt galvanic cells were obtained with a Leeds and Northrup Students' potentiometer. Other potential measurements were made with a Fairchild Model 7030 digital voltmeter. Battery discharge voltages were recorded with either a Heath EUW-20A or a Varian 9176 strip chart recorder.

Conductance Measurements

Conductance data for fused salt mixtures were obtained with an Industrial Instruments Model RC16 B2 conductivity bridge and cell. The cell constant had been previously determined to be 0.100 cm^{-1}. The cell consisted of two parts with a standard taper joint in the middle. The platinized platinum electrodes were mounted in the top and the connecting leads were sealed through the glass. The test solution was placed in the bottom part which had a flat sealed-off base, and the two parts of the cell were assembled in the dry box.

Ultraviolet and Visible Spectra

Spectra of fused salt mixtures were obtained using either a Cary 16 or Cary 118 UV-visible spectrophotometer. Spectra of fused salt mixtures in Teflon stoppered 0.1 cm cells were recorded with the Cary 16 instrument. The Cary 118 instrument was used for recording spectra of fused salt mixtures contained in the OTTLE cell.

Optically Transparent Thin Layer Electrode

An optically transparent thin layer electrochemical cell (OTTLE) similar to that described by De Angelis and Heineman (52) was constructed for use with the air sensitive fused salt mixtures. The cell is depicted in Figure 2. Corning No. 2947 microscope slides were cut in six centimeter lengths for use as cell windows. With the working, auxiliary and reference electrodes in place, the cell windows were sandwiched together using strips of two mil adhesive backed Teflon tape (Dilectrix Corp. Fluorofilm DF 1200) as spacers. The cell sides were glued and sealed with epoxy.

The reference electrode was prepared from a strip of 0.005 inch copper foil by sanding with No. 400 emery paper and washing with distilled water. Working and auxiliary electrodes were made of gold minigrid mesh of 100 wires per inch (Buckbee Mears Company) with an optical transmittance of 82%. The counter electrode was of slightly greater area than the working electrode. Before use, the OTTLE cell was rinsed successively with 6 M hydrochloric acid, 4 M nitric acid, distilled water and was then dried with a current of nitrogen. After the cell had been filled with a fused salt mixture, the open ends were sealed

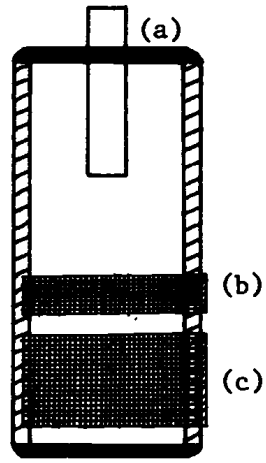

Figure 2. OTTLE cell; reference electrode,(a), working electrode,(b), and auxiliary electrode, (c).

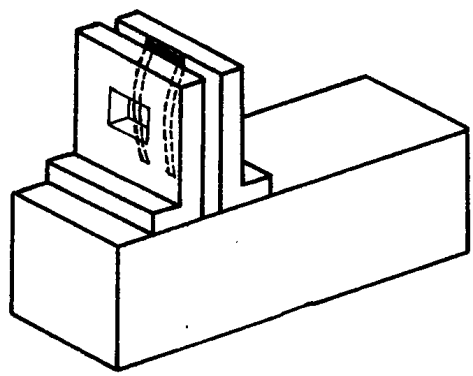

Figure 3. OTTLE spectrophotometer carriage.

with Pyseal black wax (Fisher Scientific). External electrical contacts to the protruding gold minigrid leads were made with folded strips of aluminum foil held in place by alligator clips.

An OTTLE carriage, shown in Figure 3, was designed to fit the Cary 118 spectrophotometer's sample compartment. The carriage was machined from aluminum and was anodized to be black. Tension from two bow springs held the OTTLE in place.

The OTTLE was calibrated by spectrophotometric and electrochemical methods. Coulometric data obtained from potentiostatic electrolysis of a potassium ferricyanide solution in the OTTLE was used to calculate the effective solution volume surrounding the working electrode. From electrolysis of a potassium ferricyanide solution containing potassium chloride supporting electrolyte and of a solution containing only the supporting electrolyte, plots of coulombs passed versus time were obtained. By extrapolation to t = 0 from the linear region on the plateau of the coulomb-time cures, where the cell current was mainly due to a background current, values were obtained for the number of coulombs required for electrolysis of the potassium ferricyanide-potassium chloride solution, Q, and for the supporting electrolyte alone, Q_B. The working electrode volume was calculated to be 6.65 microliters using the equation $V = (Q-Q_B)/Q_v$, where Q_v is the calculated number of coulombs required per microliter of solution of known ferricyanide concentration.

The optical path length was obtained through comparison of the absorbance of a potassium chromate solution in the OTTLE and in an accurately calibrated 1 mm cell. From the absorbance of the potassium

chromate solution at 426 nm in the OTTLE, A, and the absorbance of the same solution in the 1 mm cell, A_s, the path length, b, of the OTTLE was calculated from the equation $b = (A/A_s)b_s$, where b_s is the accurately known path length of the 1 mm cell. The OTTLE cell was found to have a path length of 0.168 mm.

Dilatometry and Viscosimetry

Test mixtures of varying composition were obtained by either dissolving additional solute in the previously examined electrolyte or preparing the electrolyte directly from triethylammonium dichlorocuprate (I) and the solute. The dilatometer used in these fluid expansion measurements was previously calibrated and described by Joedicke (53). The dilatometer is shown in Figure 4. In practice, the filled unit was immersed in a constant temperature bath to the initial stem graduation and equilibrium liquid levels of 0.00 to 1.00 ml were read at the meniscus in the stem. Liquid densities were calculated from the fluid's weight and volume, which is the sum of the bulb and stem volumes. Density measurements at temperatures precise to ± 0.1° were made at 25°, 30°, 40° and 50°C.

Fused salt viscosities were measured with a capillary viscometer similar to the Cannon-Fenske type. The viscometer is shown in Figure 5. Tygon tubing was used exclusively and the connections were wire wrapped to prevent leaks. Glycerol-water solutions for viscosity calibration were prepared using the density-viscosity data of Sheely (54, 55).

A reservoir graduation on the lower portion of the viscometer was used to insure that reproducible volumes of liquids were introduced.

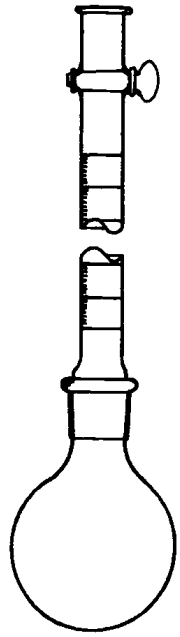

Figure 4. Dilatometer

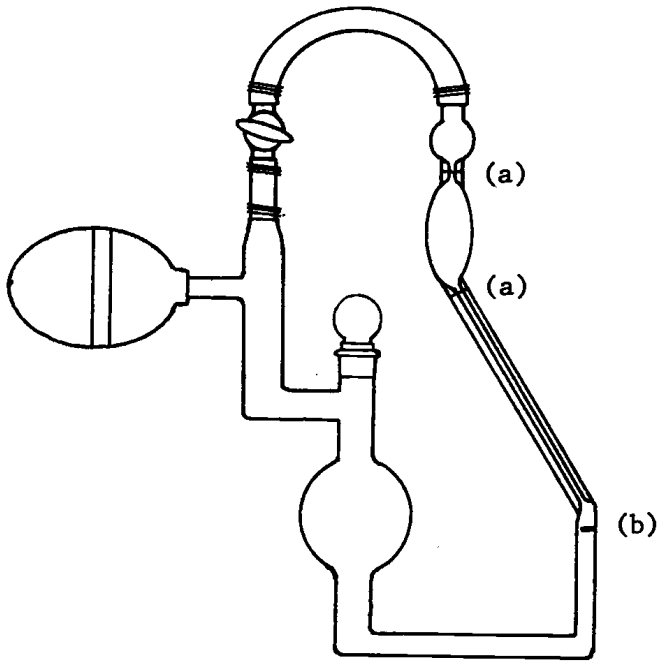

Figure 5. Viscometer; efflux marks, (a), fill mark, (b).

With the system airtight, and the stopcock closed, liquid could be forced into the upper reservoir by application of pressure to the pipet bulb. When the desired amount of liquid had been transferred, the stopcock was opened allowing flow into the lower reservoir to commence. Liquid efflux times were measured between two marks at opposite ends of the upper reservoir.

The same fused salt mixtures prepared for conductance studies were used in viscosity measurements.

Analytical Methods

Iron in Potassium Hexacyanoferrate(III)

The potassium hexacyanoferrate(III) solution, used in the calibration of the OTTLE, was standardized as follows. Iron was determined by the titrimetric method described by Ingram (56). A weighed portion of potassium ferricyanide was dissolved in water and reduced to ferrocyanide with stannous chloride. The ferrocyanide was then titrated with a solution of 0.1000 N potassium dichromate. The standard potassium dichromate solution was prepared by dissolving 4.9024 gram NBS SRM 136b (oxidimetric purity: 99.98%) in water and diluting to 1 liter. The titrimetric endpoint was easily observed as a colorless to violet solution transition due to the diphenylamine sulfonate indicator.

Lithium Chloride in Triethylammonium Dichlorocuprate(I)

A portion of the lithium chloride-triethylammonium dichlorocuprate (I) suspension was filtered through a medium porosity glass frit, weighed, and dissolved in 8 M nitric acid. The solution was

appropriately diluted with distilled water and analyzed by flame emission with an Instrumentation Laboratory 351 AA/AE spectrophotometer.

Analysis of Copper in a Fused Salt Mixture

Copper in triethylammonium dichlorocuprate(I) saturated with excess triethylammonium chloride was determined using atomic absorption spectroscopy. A filtered, weighed portion of the liquid was digested in nitric and sulfuric acids until the mixture fumed. After cooling, the acidic residue was diluted with distilled water and analyzed. An NBS copper-nickel-zinc reference alloy was simultaneously analyzed to insure the accuracy of the overall procedure.

IV. PHYSICOCHEMICAL STUDIES OF THE ROOM TEMPERATURE FUSED SALT TRIETHYLAMMONIUM DICHLOROCUPRATE(I) AND OF SOLUTIONS OF VARIOUS SALTS IN IT

Spectroscopic Studies

Typical spectra (versus air in the reference beam) in the 360 to 700 nm region of triethylammonium dichlorocuprate(I) and of a solution of copper(II) chloride in it are shown in Figure 6. Neat triethylammonium dichlorocuprate(I) is pale yellow in appearance, but thin films of it show no absorption maximum above 300 nm. Its light yellow color is due to the visible tail of an intense charge transfer absorption in the ultraviolet. Solutions of copper(II) chloride in triethylammonium dichlorocuprate(I) absorb more strongly across the visible region. If a sample of the solution is thick or concentrated it appears black. With low concentrations and short pathlengths, the color is seen to be deep green.

The spectrum of a solution of copper(II) chloride in triethylammonium dichlorocuprate(I) as solvent, versus the neat solvent in the reference beam, does result in an absorption peak, as shown in Figure 7. Spectra of such solutions with the neat fused salt as reference seem to obey Beer's Law at concentrations up to at least 0.1 M. For example, in Figure 8, the absorbance at 600 nm is seen to be a linear function of copper(II) concentration. The absorbances of the three solutions containing the lowest copper(II) concentrations do appear to be a little high, presumably due to slight oxygen contamination of the parent solution from which they were prepared. The calculated molar absorptivity

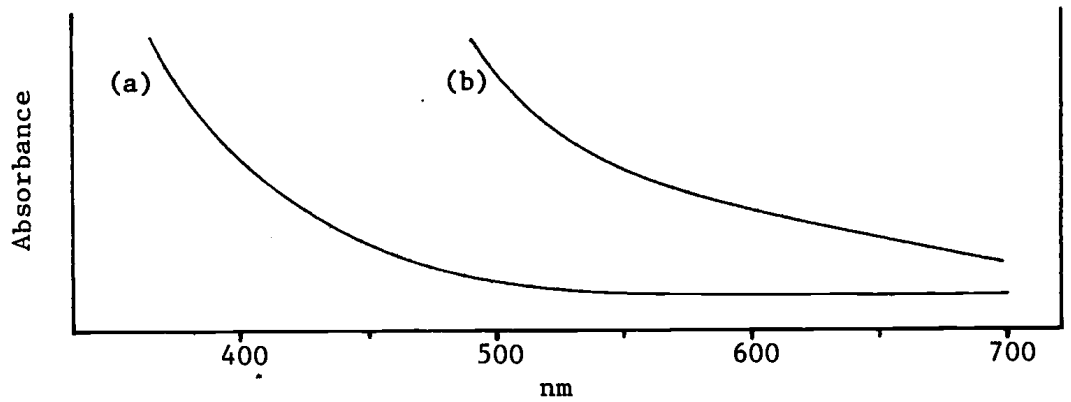

Figure 6. Typical spectra of triethylammonium dichlorocuprate(I), (a); and of a solution of $CuCl_2$ in it, (b), versus air.

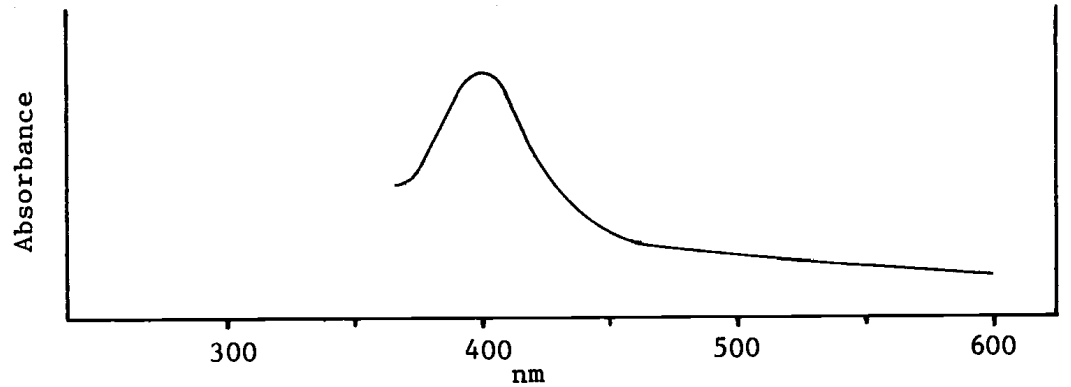

Figure 7. Typical spectrum of $CuCl_2$ in triethylammonium dichlorocuprate(I) with triethylammonium dichlorocuprate(I) in the reference path.

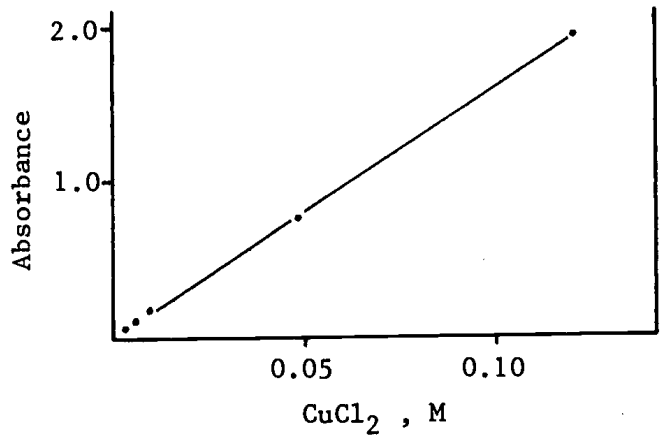

Figure 8. Absorbance of $CuCl_2$ in triethylammonium dichlorocuprate(I) at 600 nm, corrected for solvent absorbance.

(extinction coefficient) of dissolved copper(II) chloride at 600 nm was 167 lit $mol^{-1}cm^{-1}$. Similarly, it was found to be 2019 lit $mol^{-1}cm^{-1}$ at the wavelength of maximum absorbance, 402 nm.

Densities

Density data for triethylammonium dichlorocuprate(I) and for fused salt mixtures at several temperatures are listed in Table 1. All these electrolytes had cubic coefficients of expansion of 1.00056 to 1.00060°C^{-1}.

The room temperature densitites, and molar volumes calculated from them are, respectively, 4.14 g/cc and 23.9 cc/mol for solid copper(I) chloride, 1.069 g/cc and 128.8 cc/mol for solid triethylammonium chloride, and 1.398 g/cc and 169.3 cc/mol for liquid triethylammonium dichlorocuprate(I). The molar volume of the fused salt exceeds the molar volumes of its solid constituents by 10.9%, corresponding to the expansion taking place during the markedly endothermic reaction

Table 1. Densities of fused salt mixtures at various temperatures.

Electrolyte[a]			Density[b]			
CuCl	Et_3NHCl	$CuCl_2$	25°C	30°C	40°C	50°C
0.500	0.500	0	1.398	1.394	1.386	1.378
0.472	0.472	0.0558	1.443	1.439	1.431	1.422
0.446	0.446	0.109	1.522	1.517	1.509	1.501
0.570	0.430	0	1.519	1.515	1.506	1.497
0.624	0.376	0	1.627	1.622	1.613	1.603
0.667	0.333	0	1.743	1.738	1.729	1.720

[a] mole fraction of components

[b] g/cm^3

$$CuCl_{(c)} + Et_3NHCl_{(c)} \rightarrow Et_3NHCuCl_2 \quad (1)$$

The greater densities of copper(I) and copper(II) chlorides than of triethylammonium dichlorocuprate(I) account for the correspondence between increasing concentrations of these salts and the densities of fused salt mixtures containing them.

Conductivities

The effect of temperature on the specific conductances of fused salt mixtures containing copper(II) chloride is shown in Figure 9. Specific conductances were measured at 25°, 30°, 40°, and 50°C ± 0.1°. Successive solutions of a series of fused salt mixtures were prepared by dissolving additional solute (e.g., triethylammonium chloride, copper(II) chloride) in the previously examined electrolyte. Other mixtures were prepared directly from triethylammonium dichlorocuprate(I) and the solute. Figure 10 shows the temperature variation in specific conductance of fused salt mixtures containing excess copper(I) chloride. Isotherms in Figures 11 and 12 demonstrate the effects of compositional changes on specific conductance. All salts added to triethylammonium dichlorocuprate(I), including lithium chloride, resulted in mixtures of lower conductances at 25°C. Thus, while the observed specific conductance of neat triethylammonium dichlorocuprate(I) at 25°C was 4.30×10^{-3} $ohm^{-1}cm^{-1}$, the specific conductance of triethylammonium dichlorocuprate (I) saturated with lithium chloride (0.07 m) was found to be 3.68×10^{-3} $ohm^{-1}cm^{-1}$. Another lithium chloride saturated fused salt mixture, containing copper(I) chloride and triethylammonium chloride in a mole ratio of 1.5 to 1.0, had a specific conductance of $2.76 \times 10^{-3} ohm^{-1}cm^{-1}$ at 25°C.

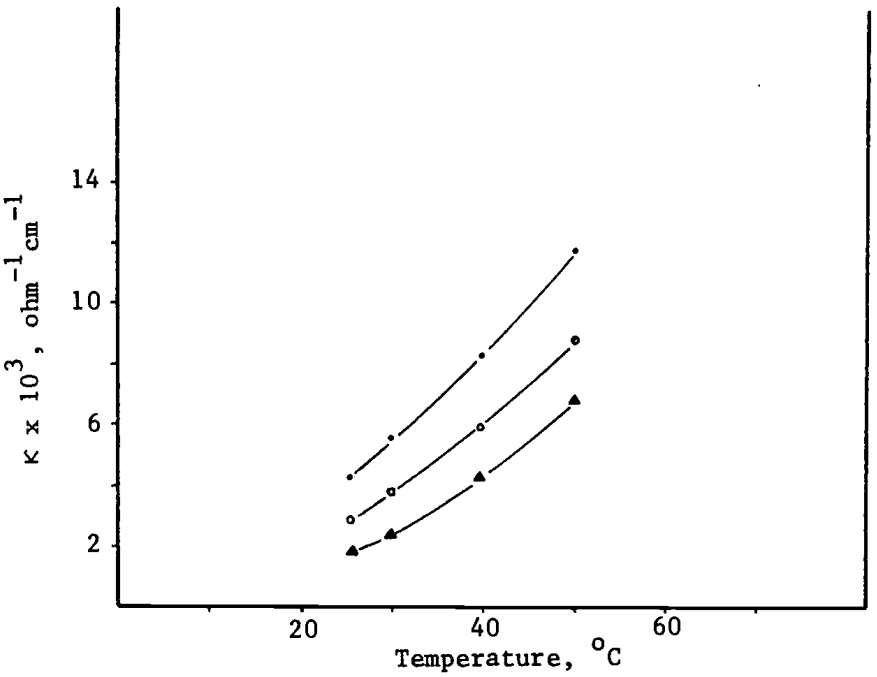

Figure 9. Specific conductance of solutions of $CuCl_2$ in triethylammonium dichlorocuprate(I). Mole fraction Et_3NHCl-CuCl-$CuCl_2$: (•), 0.5-0.5-0; (o), 0.472-0.472-0.0558; (▲), 0.446-0.446-0.109.

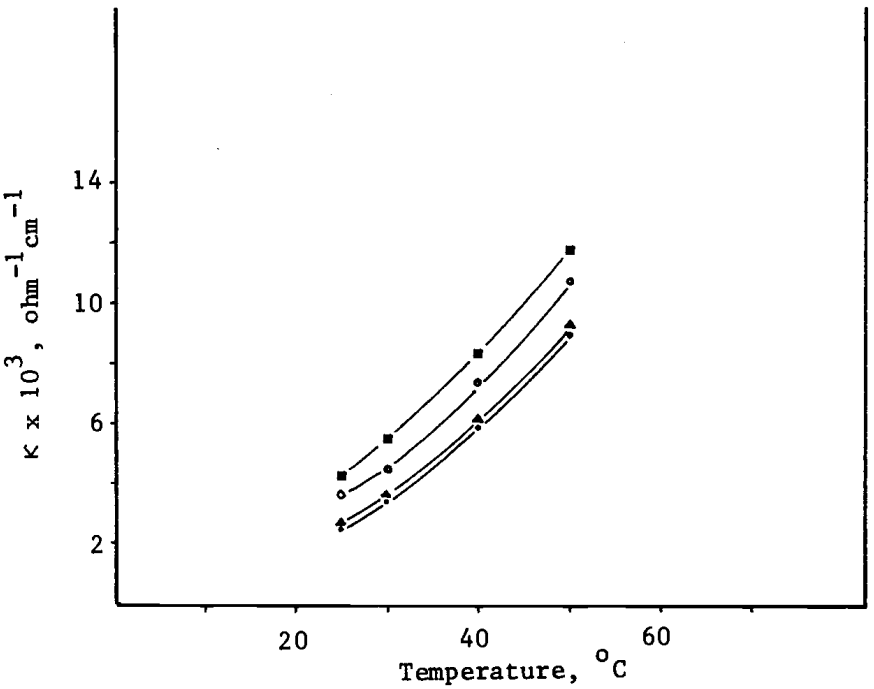

Figure 10. Specific conductance of solutions of CuCl in triethylammonium dichlorocuprate(I). Mole fraction Et_3NHCl-CuCl: (■), 0.5-0.5; (o), 0.430-0.570; (▲), 0.376-0.624; (•), 0.333-0.667.

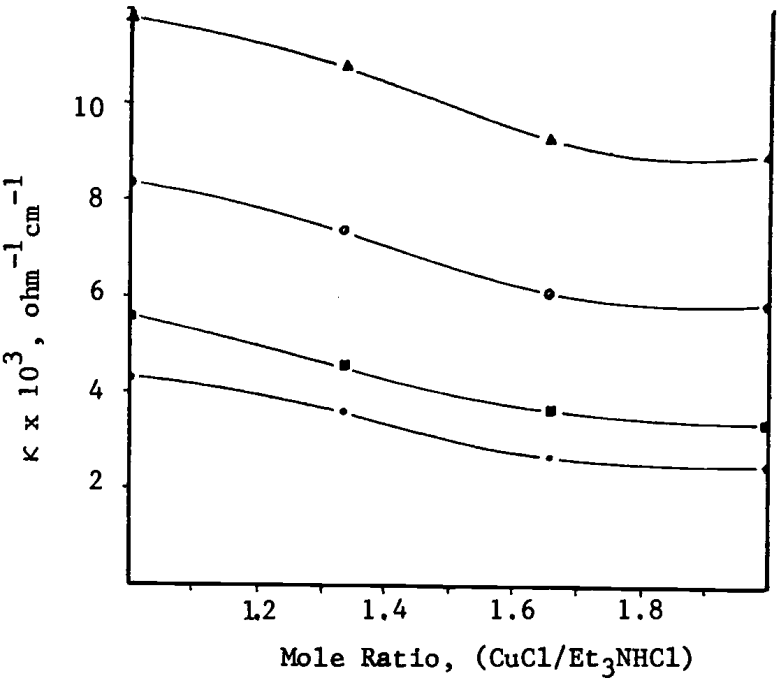

Figure 11. Specific conductance of solutions of CuCl in triethylammonium dichlorocuprate(I) at various temperatures; (•), 25°; (■), 30°; (o), 40°; (▲), 50°.

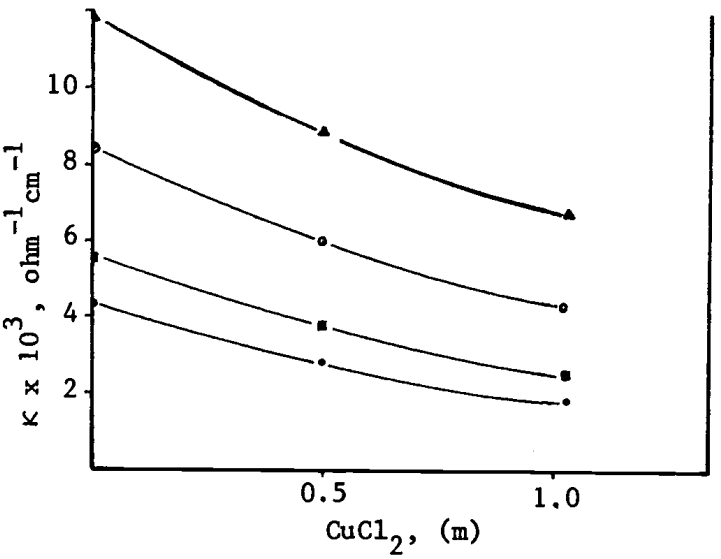

Figure 12. Specific conductance of solutions of $CuCl_2$ in triethylammonium dichlorocuprate(I) at various temperatures; (•), 25°, (■), 30°, (o), 40°, (▲), 50°.

The specific conductance of triethylammonium dichlorocuprate(I) saturated with triethylammonium chloride was found to be 3.74×10^{-3} ohm^{-1}cm^{-1}. The mole ratio of copper(I) chloride to triethylammonium chloride in the saturated solution was 1.00 to 1.04, respectively.

The specific conductance, at 25°C, of neat triethylammonium dichlorocuprate(I) observed in this work is slightly higher than the value reported earlier, 3.84×10^{-3} ohm^{-1}cm^{-1} (3). This difference may be partially due to temperature induced changes in the fused salt structure brought about during the temperature-conductivity studies.

The relationship between equivalent conductance and temperature has been shown both experimentally and theoretically to follow the equation $\Lambda = A\, e^{-E_\Lambda/RT}$ for a number of fused salt systems (23, 24, 25). This Arrhenius-type equation represents an approximation to a more rigorous expression which would consider individual activation energies of all cationic and anionic conducting species. However, the simplified equation is applicable when the activation energies of all conducting species are very similar or that of one species much less than the others. Curve A of Figure 13 shows that triethylammonium dichlorocuprate(I) exhibits approximate Arrhenius type behavior; its log Λ vs. 1/T plot is nearly linear. Fused salt mixtures containing copper(II) chloride (curves b and c) and mixtures containing copper(I) chloride (curves d, e, and f) also show only slight deviations from Arrhenius-type behavior. These deviations from linearity may result from activation energy complications, mentioned above, or temperature dependent equilibria between ions, ion pairs and molecular constituents.

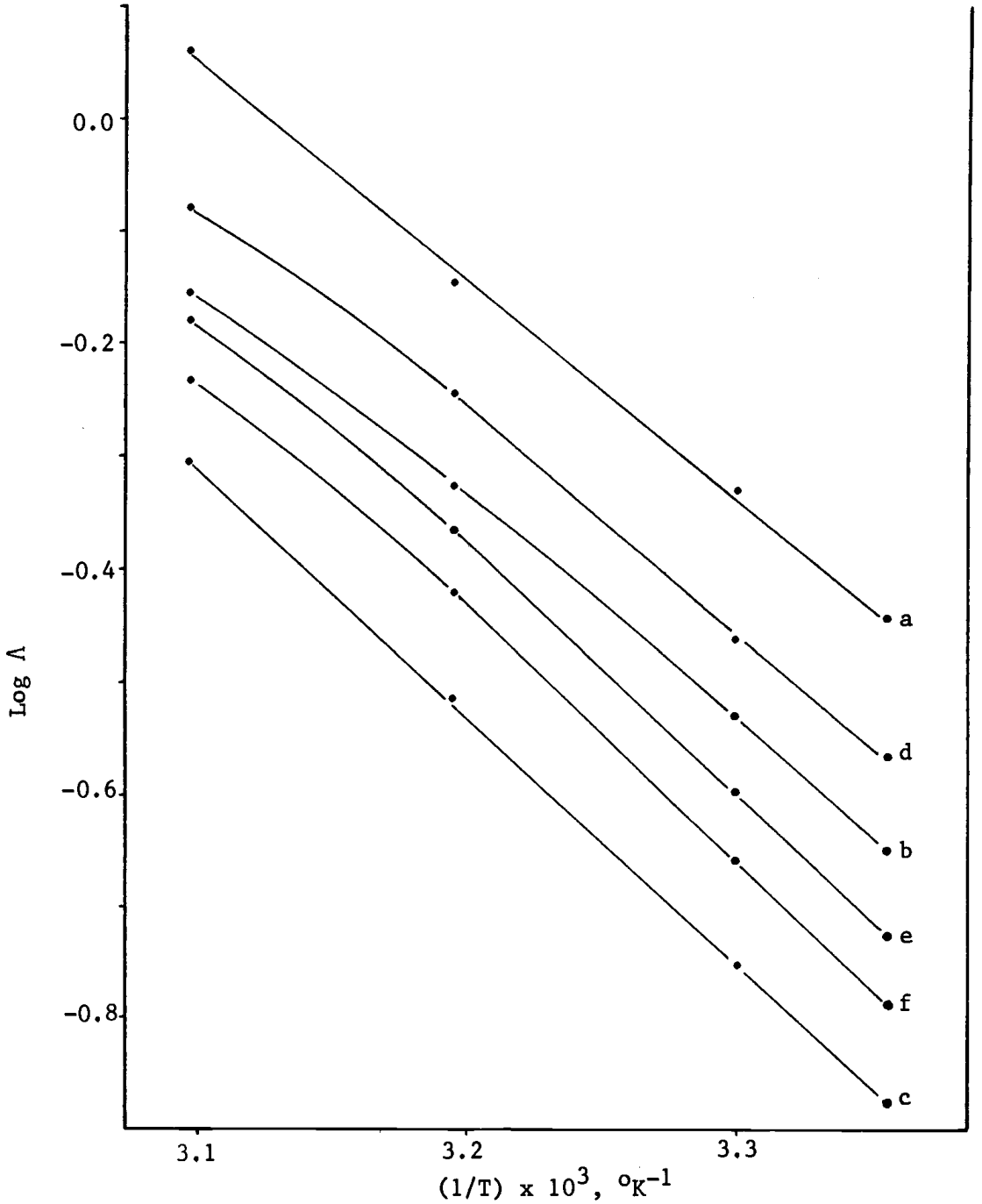

Figure 13. Log Λ vs. 1/T for solutions of CuCl and $CuCl_2$ in triethylammonium dichlorocuprate(I). Mole fraction Et_3NHCl-CuCl-$CuCl_2$: (a), 0.5-0.5-0; (b), 0.472-0.472-0.0558; (c), 0.446-0.446-0.109; (d), 0.430-0.470-0; (e), 0.376-0.624-0; (f), 0.333-0.667-0.

Viscosities

Variations in viscosities of several fused salt mixtures as a function of temperature are shown in Figure 14. Variations in viscosity of solutions of copper(I) and copper(II) chlorides in triethylammonium dichlorocuprate(I) as a function of composition are shown in Figures 15 and 16.

The linear relationships observed in Figure 17 indicate an Arrhenius-type equation for viscosity, $\eta = A\ e^{-E_\eta/RT}$, to be followed for all fused salt mixtures.

Discussion

The visible spectrum of a solution of copper(II) chloride in triethylammonium dichlorocuprate(I) as solvent, with the neat solvent in the reference beam, or versus air corrected for the absorption of the solvent, shows an absorption peak at 402 nm. This value is in fair agreement with the work done at Hampden-Sydney College and reported by Porterfield; those workers found the maximum at 424 nm. A variety of copper(II) complexes with chloride ions or other chlorospecies as ligands are known and their spectra have been discussed by Hatfield and Piper (16). For example, square planar $CuCl_4^{2-}$ absorbs at 407 nm. These absorptions are assigned to ligand to metal charge transfer. It is important that the copper(II) absorption is found to obey Beer's law, as this will permit the application of spectroscopic measurements to the determination of copper(II) concentrations in the coulometric studies to be discussed in Section V, Fused Salt Potentiometry and Coulometry. It also indicates that, whatever the actual copper(II)

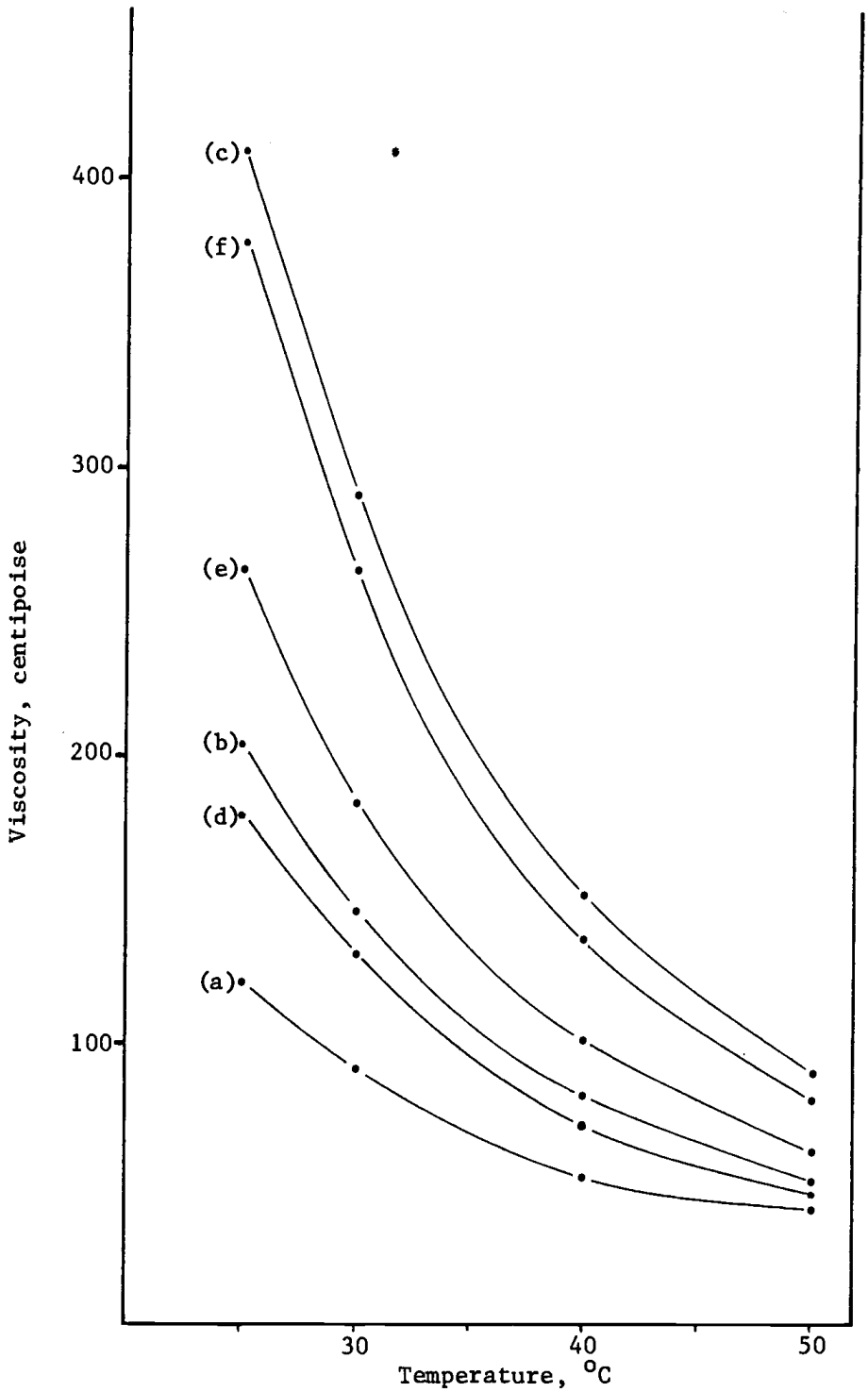

Figure 14. Viscosity of solutions of CuCl and $CuCl_2$ in triethylammonium dichlorocuprate(I) at various temperatures. Mole fraction Et_3NHCl-CuCl-$CuCl_2$: (a), 0.5-0.5-0; (b), 0.472-0.472-0.0558; (c), 0.446-0.446-0.109; (d) 0.430-0.570-0; (e), 0.376-0.624-0; (f), 0.333-0.667-0.

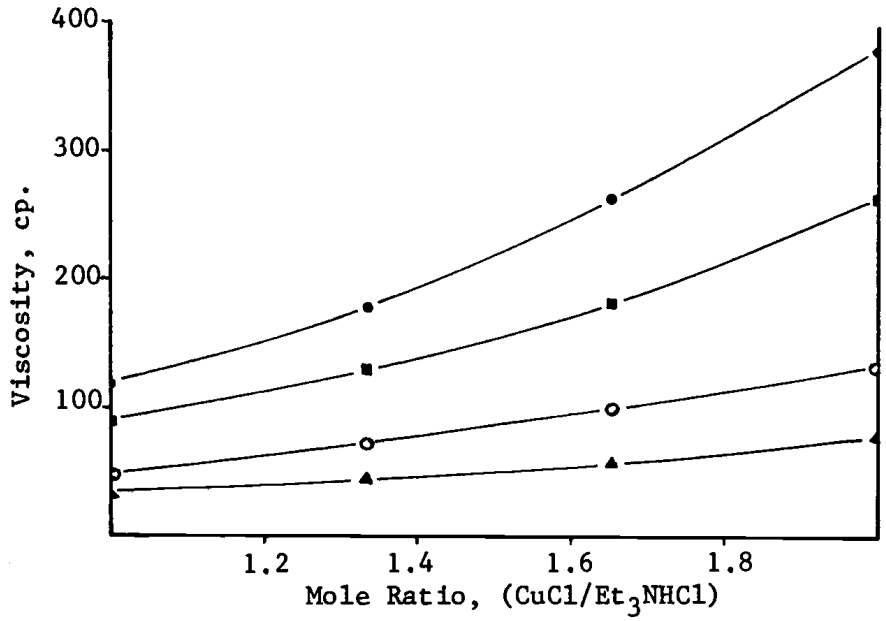

Figure 15. Viscosity of solutions of CuCl in triethylammonium dichlorocuprate(I) at various temperatures; (●), 25°; (■), 30°; (o), 40°; (▲), 50°.

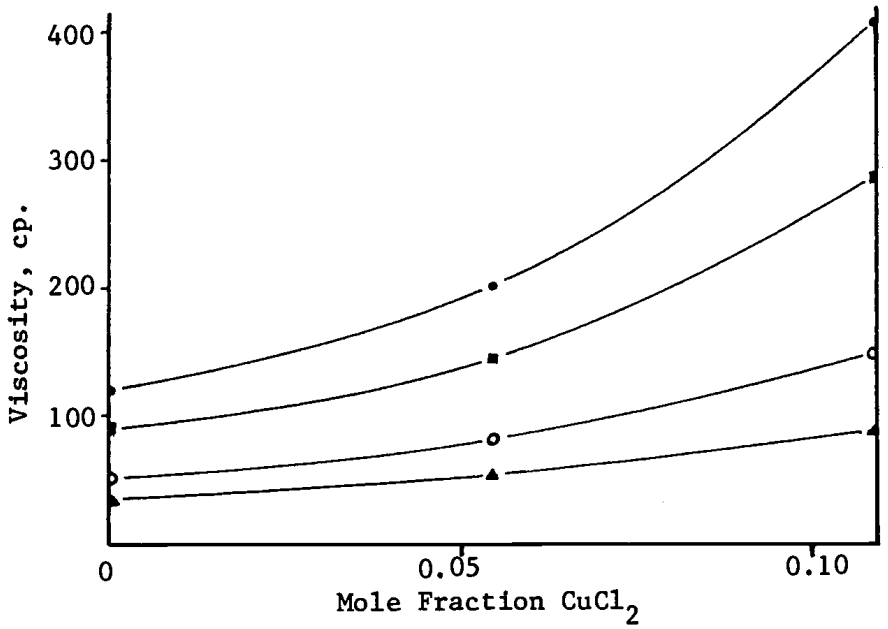

Figure 16. Viscosity of solutions of $CuCl_2$ in triethylammonium dichlorocuprate(I) at various temperatures; (●), 25°; (■), 30°; (o), 40°; (▲), 50°.

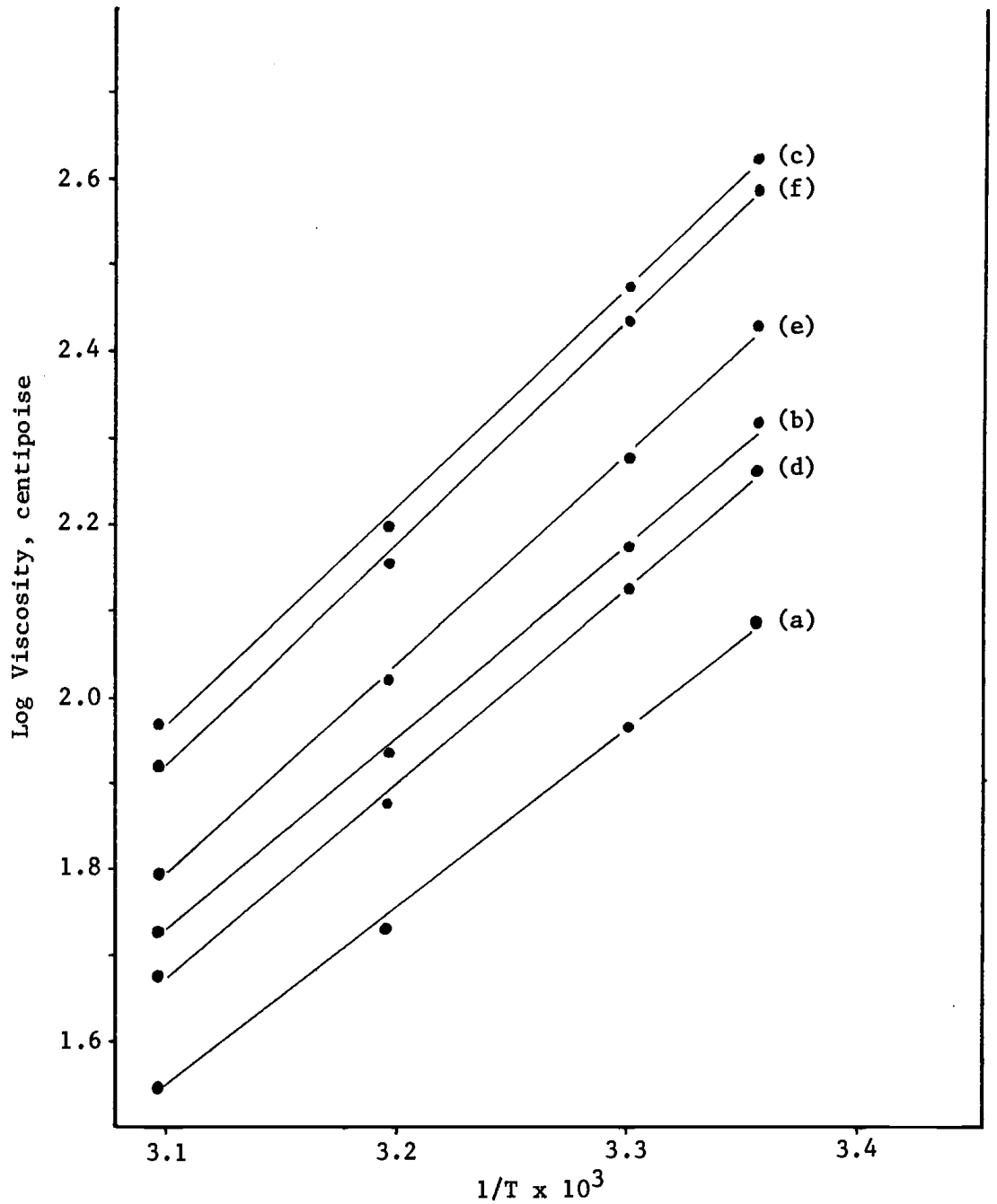

Figure 17. Plot of $\log(\eta)$ versus 1/T for solutions of CuCl and $CuCl_2$ in triethylammonium dichlorocuprate(I). Mole fraction Et_3NHCl-CuCl-$CuCl_2$: (a), 0.5-0.5-0; (b), 0.472-0.472-0.0558; (c), 0.446-0.446-0.109; (d), 0.430-0.570-0; (e) 0.376-0.624-0; (f), 0.333-0.667-0.

containing species are in the chlorocuprate(I) solvent system, the nature of these species from an electronic spectroscopic viewpoint is independent of copper (II) concentration within the range studied.

It is of interest to consider the conductivity and viscosity data together, since the mobility of a charge carrier depends in part on bulk viscosity and since the mechanisms of both phenomena and their temperature dependencies are related. Average activation energies for viscous flow, E_η, conductance E_Λ, and their ratios, calculated from least squares slopes in Figures 13 and 17 are shown in Table 2. The activation energies for viscous flow, 9.6-11.8 kcal/mole, are in the range generally found for fused salts (26). However, the activation energies for conductance are about three times larger than generally observed. In addition, the ratio, E_η/E_Λ, has been found to vary between 2 and 7 for other fused salts (30). For all triethylammonium dichlorocuprate(I) mixtures studied a considerably lower ratio of 1.2 was observed.

Table 2. Activation energies for conductance and viscous flow.

Electrolyte[a]			Activation Energy[b]		
CuCl	Et_3NHCl	$CuCl_2$	E_η	E_Λ	E_η/E_Λ
0.500	0.500	0	9.6	7.8	1.23
0.472	0.472	0.0558	10.4	8.6	1.21
0.446	0.446	0.109	11.6	10.0	1.16
0.570	0.430	0	10.4	8.6	1.21
0.624	0.376	0	11.2	9.6	1.17
0.667	0.333	0	11.8	9.8	1.20

[a] mole fraction of each component

[b] kcal/mole

The Walden equation, $\eta\Lambda$ = const., is not followed very well by the fused salt mixtures as evidenced by a 20-30% variation in the product in the temperature range 25-50°C. The Walden product rule is generally not obeyed by fused salts (31). The data in Table 3 show that the relationship proposed by Frenkel (32), $\eta\kappa^{(E_\eta/E_\Lambda)}$ = const., is more closely followed by liquid triethylammonium dichlorocuprate(I) mixtures.

These results indicate that energy barriers encountered in mass flow are greater than those involved in ionic migration, in agreement with data for other fused salts. The nearness of the ratio, E_η/E_Λ, to unity indicates how closely the processes of ionic transfer and mass flow are related to the same factors. These processes are apparently more closely related in triethylammonium dichlorocuprate(I) mixtures than in most other fused salts.

Table 3. Effect of temperature on Frenkel's viscosity-conductance function applied to fused salt mixtures.

Electrolyte[a]						
CuCl	Et_3NHCl	$CuCl_2$	25°C	30°C	40°C	50°C
0.500	0.500	0	0.150	0.155	0.150	0.151
0.472	0.472	0.0558	0.174	0.174	0.176	0.172
0.446	0.446	0.109	0.288	0.282	0.280	0.285
0.570	0.430	0	0.202	0.195	0.198	0.196
0.624	0.376	0	0.267	0.266	0.270	0.260
0.667	0.333	0	0.297	0.300	0.300	0.289

[a] mole fraction of components

V. OVERPOTENTIAL AND RELATED STUDIES OF ELECTRODES IN ROOM TEMPERATURE FUSED SALTS

The Copper-Triethylammonium Dichlorocuprate(I) Reference Electrode

A practical reference electrode for electrochemical investigations of triethylammonium dichlorocuprate(I) fused salt mixtures should be stable, reproducible, not easily polarized and operate without a salt bridge. Additionally, if a reference electrode of the first kind (M/M^{n+}) is chosen, the potential determining solute species and the metal electrode should be inert towards fused salt mixtures. The latter requirement imposes a considerable restriction on the choice of a reference electrode in light of possible copper(I) and copper(II) redox reactions with such a system.

These requirements were found to be adequately satisfied by the copper-triethylammonium dichlorocuprate(I) half cell and unless specified otherwise, all metal-fused salt interfacial potentials were measured with respect to it. With the exception that copper(II) species in the fused salt solution are reduced, presumably to copper(I), by metallic copper, this type of reference half cell was found to perform well in a variety of experimental conditions. Copper reference electrodes were pre-treated with 8 M nitric acid, polished with No. 400 emery paper, and washed with distilled water.

Using the cell: Hg, Hg_2Cl_2, KCl (aq. satd.)/$Et_3NHCuCl_2$/$Et_3NHCuCl_2$/Cu in the design shown in Figure 18, the operational potential of the fused salt reference electrode plus junction potential was found to be reproducible and steady. This operational potential was found to be

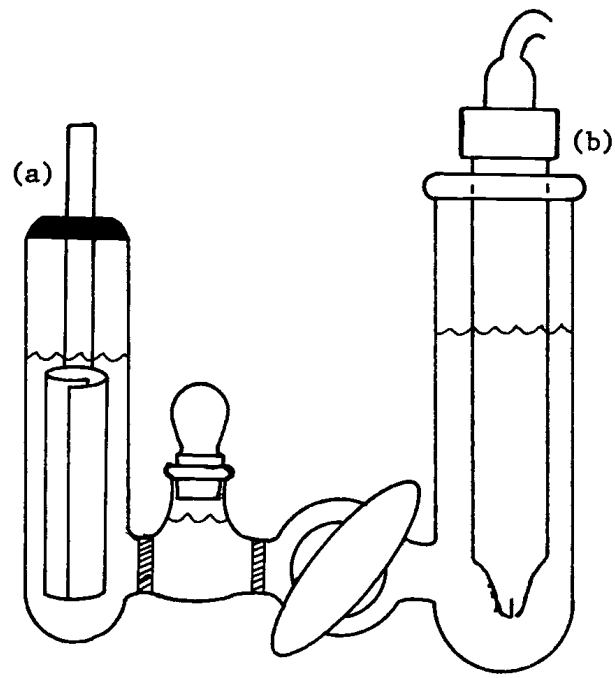

Figure 18. Cell used to measure the potential of the $Cu/Et_3NHCuCl_2$ reference electrode with respect to the SCE; (a), copper foil electrode; (b), SCE.

0.242 volt at 30°C, 0.241 volt at 25°C, and 0.238 volt at 20°C. This places it at very close to zero on the normal hydrogen potential scale.

Electrode polarizability was studied by galvanostatic perturbation of the equilibrium potential. The following three electrode arrangement was used to study the effects of polarizing current on the rest potential stability of the copper-triethylammonium dichlorocuprate(I) reference electrode. Triethylammonium dichlorocuprate(I) was added to a cell which contained identical 11 gauge copper wire working, auxiliary and reference electrodes. The area of the working electrode was approximately 1 cm^2. A length of glass tubing shielded the reference electrode from most of the bulk electrolyte, but allowed electrical contact with the solution through an open end.

Resultant potential-time curves for an 11 gauge wire electrode are shown in Figure 19. The curves indicate the time necessary for equilibrium potential restoration and the extent to which reference potentials will be altered by anodic and cathodic current passage. Polarization of the 1 cm^2 electrode varied considerably over the range of currents studied and indicates that instrumentation with input impedences of less than 10^6 ohms should be used with caution.

Experimental observations have shown that copper(II) species formed on the surface layer of triethylammonium dichlorocuprate(I) by air oxidation, will alter the rest potential by several millivolts.

Fused Salt Potentiometry and Coulometry

Potential measurements on galvanic cells of the type

$$Cu/Et_3NHCuCl_2/Et_3NHCuCl_2,\ CuCl_2\ (M)/Pt$$

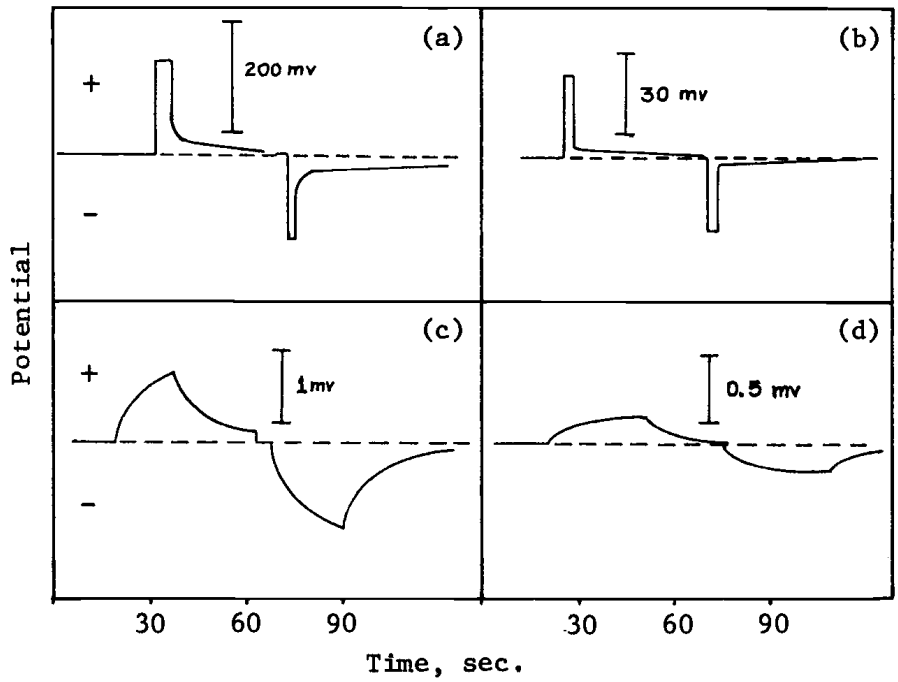

Figure 19. Polarization of a copper wire reference electrode at several currents. Electrode currents were discontinued at anodic and cathodic polarization maxima; (a), 1 ma; (b), 100 μa; (c), 1 μa; (d), 0.1 μa.

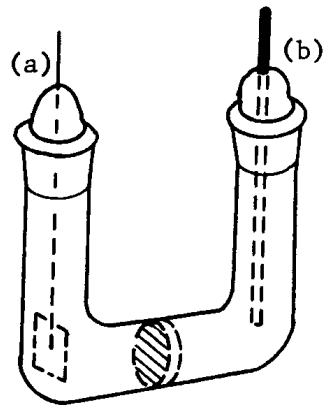

Figure 20. Cell used for EMF measurements on galvanic cells of the type:
$Cu/Et_3NHCuCl_2/Et_3NHCuCl_2$, $CuCl_2$ (M)/Pt
Platinum electrode, (a); copper electrode, (b).

were obtained at 25°C using the cell described in Figure 20. The cell was constructed from Pyrex 10/18 standard taper joints and a medium porosity glass frit. Each half cell had a volume of approximately 4.5 cm^3. The reference copper electrode was fashioned from 11 gauge wire and prepared for use as previously described. The redox electrode consisted of a 1 cm^2 piece of platinized platinum foil. Treatment of the redox electrode before use involved washing with 8 M nitric acid, distilled water, and drying.

Potentials obtained from the cell described above and from the OTTLE

$$Cu/Et_3NHCuCl_2/Et_3NHCuCl_2,\ CuCl_2\ (M)/Au$$

are shown in Figure 21. OTTLE voltages were obtained at 21°C (ambient temperature), but have been corrected to 25°C using the Nernst equation. The OTTLE voltages, which were corrected 1-2 mv, were included in Figure 21 to emphasize the difference in slopes for data in the regions above and below about 0.55 v. As a working definition, the copper electrode

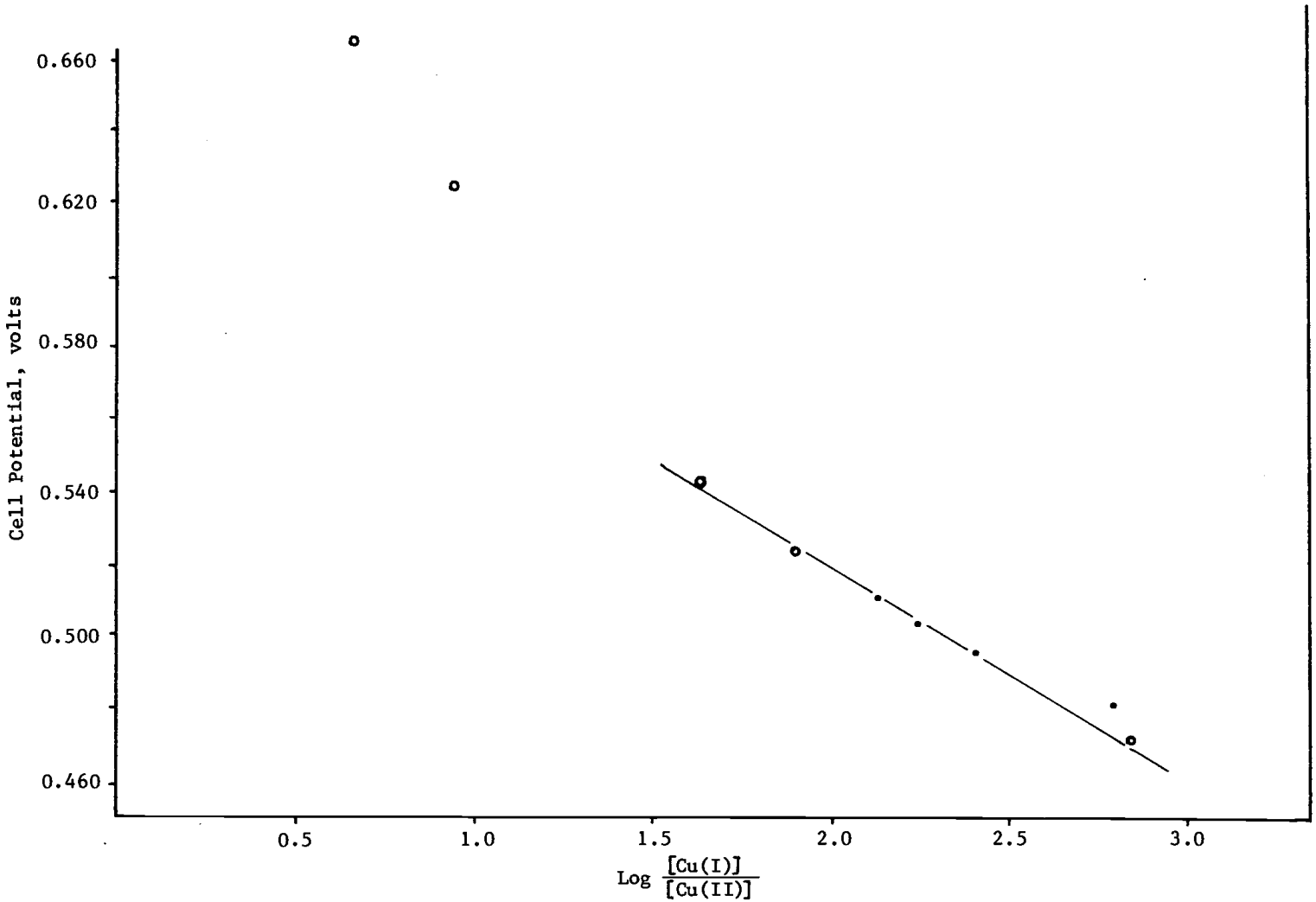

Figure 21. Potential of fused salt galvanic cell as a function of $[CuCl_2]$; (o-o-o), galvanic cell (figure 20); (●-●-●), OTTLE cell.

in these cells is assigned a potential of zero volts so the cell EMF is related to the ratio of oxidized and reduced forms of copper in the redox half cell; $E_{cell} = E_{ref.} + E_{junction} + E_{redox}$.

The theoretical Nernstian slope at 25°C is 59.16 mv/decade. The least squares slope of the line through the experimental points in Figure 21, calculated from data between 0.47 and 0.55 v, is 55.1 mv/decade. Thus, while a Nerstian type behavior is observed for lower concentrations of copper(II), higher concentrations exhibit non-ideal behavior.

The magnitude and sign of the liquid junction potential in these cells are indeterminable since neither the abundances of ionic species nor their mobilities are known. Diffusion potential effects along with changes in activity coefficients and equilibria between complex species are presumably responsible for the curvature seen in Figure 21 above 0.14 M copper(II).

Galvanostatic electrolysis of triethylammonium dichlorocuprate(I) in conjunction with spectrophotometric measurement of the anodic product (Figure 22), using the OTTLE cell, indicates the electrochemical reaction to be

$$\text{anode:} \quad Cu(I) \rightarrow Cu(II) + e^-$$

$$\text{cathode:} \quad Cu(I) + e^- \rightarrow Cu(0)$$

Electrochemical n values for the reaction which occurred at 0.61 v vs. the copper reference electrode, were calculated from the absorption of partially electrolyzed fused salt mixtures using the known extinction coefficient of copper(II) chloride. Electrochemical n values for five consecutive partial anodic electrolyses of the same solution were 1.50,

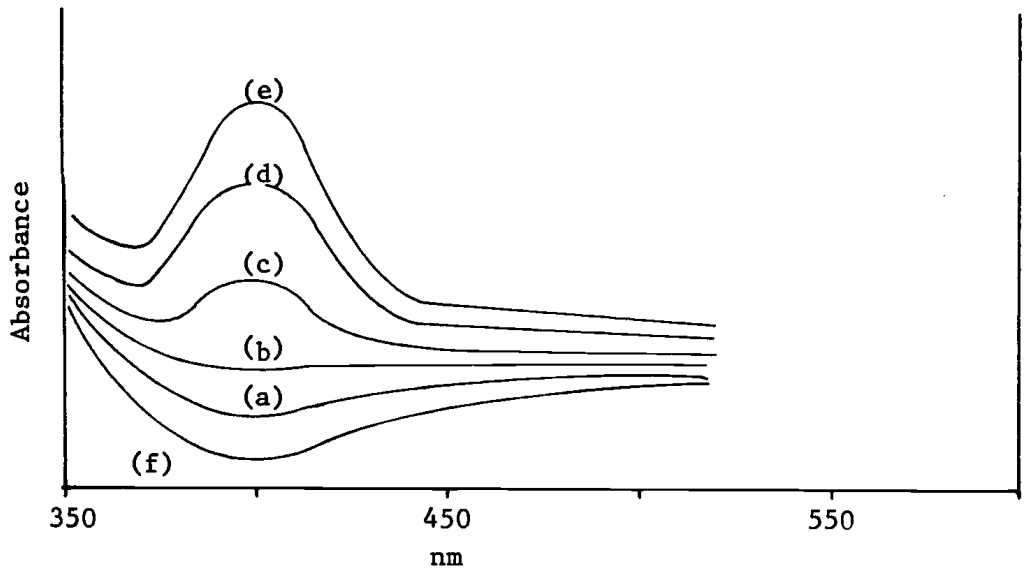

Figure 22. Spectra of electrogenerated Cu(II) in triethylammonium dichlorocuprate(I); (a), $5x10^{-3}$coul.; (b), 10^{-2}coul.; (c), $2x10^{-2}$coul.; (d), $3x10^{-2}$coul.; (e), $4x10^{-2}$coul., (f), 0 coul.

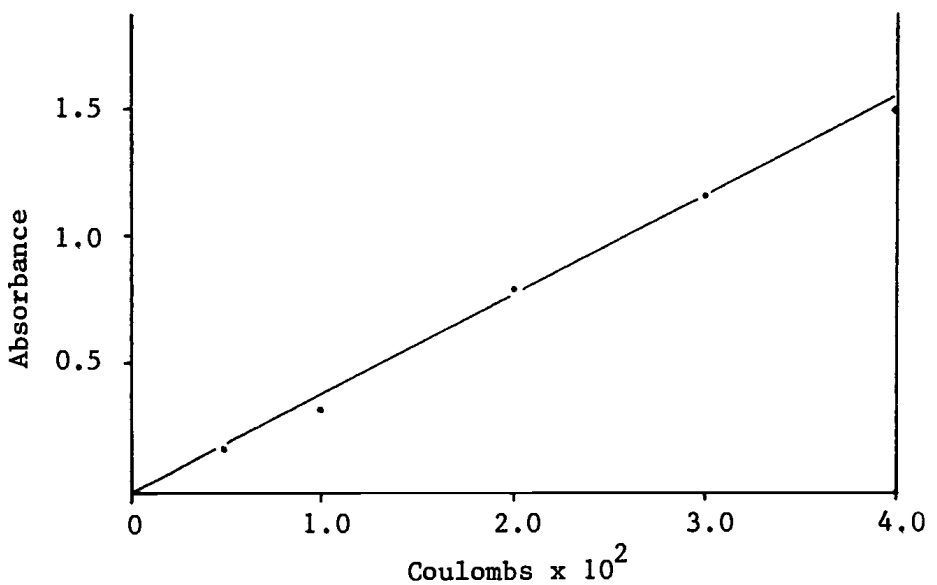

Figure 23. Absorbance of electrogenerated Cu(II), at 402 nm, in the OTTLE cell.

1.62, 1.33, 1.36, and 1.42, which results in an average of 1.45. The absorbance of electrogenerated copper(II) in the OTTLE as a function of coulombs passed through the cell is shown in Figure 23. As a result of high electrolyte resistance, galvanostatic currents of much greater than the 5 μa carried in this experiment resulted in non-uniform distribution of the anodic product over the minigrid surface. Obtaining an anodic product which was uniformly distributed over the optically transparent electrode was of great importance for Beer's law to be applicable because the collimated light source in the spectrophotometer did not pass through quite half the electrode area of 3.4 x 11.4 mm. Background currents due to minute quantities of impurities in the triethylammonium chloride or copper(I) chloride may have contributed significantly to the cell current. Successive electrolyses of 0.01 coulomb were obtained in this experiment and each required in excess of 40 minutes. During this time some of the electrogenerated copper(II) diffused away from the edges of the working electrode. Considering the lengthy times required for electrolysis and possibly some inefficiency in the coulometry an n value above one would be expected.

Comparison of the spectra of copper(II) chloride in triethylammonium dichlorocuprate(I) and of the electrogenerated anodic product indicates the solutes in both solutions to be the same. The electrochemical n value similarly reinforces this conclusion.

Potentials developed between the copper reference and gold auxiliary electrodes of the OTTLE were observed before and after coulombic studies. The potential measured before any electrolysis was considerably larger than that observed after current had passed through the

cell, indicating copper metal to be the cathodic product. Further evidence that copper metal is the cathodic product of electrolysis of this type of cell comes from charging experiments with fused salt batteries where copper metal deposits were visually in evidence, and which will be discussed in Section VI.

Voltage Sweep Studies

Bipolar potential scans in neat triethylammonium dichlorocuprate(I) were obtained using a cell with a platinum or galssy carbon working electrode, a copper reference electrode, and platinum auxiliary electrode. Sweeps at anodic and cathodic polarization rates of 2-10 mv/second were carried out in unstirred solutions using a conventional three electrode potentiostat. A platinum wire working electrode, approximately 0.1 cm^2 in area, was prepared by lightly polishing it with No. 400 emery paper, and washing it with 8 M nitric acid and distilled water. The flat circular glassy carbon electrode employed had an approximate surface area of 0.02 cm^2 and was prepared by washing it with 4 M nitric acid and distilled water. An auxiliary electrode was fashioned from a length of platinum wire of greater surface area than either working electrode. The 11 gauge copper wire reference electrode was partially shielded from the bulk electrolyte by a length of glass tubing open at the bottom.

Cyclic voltage sweeps of triethylammonium dichlorocuprate(I) provide evidence for at least two anodic reactions. A typical cyclic scan obtained at 21°C is shown in Figure 24(a). The general features of these voltammetry curves are reproducible, but peak currents and

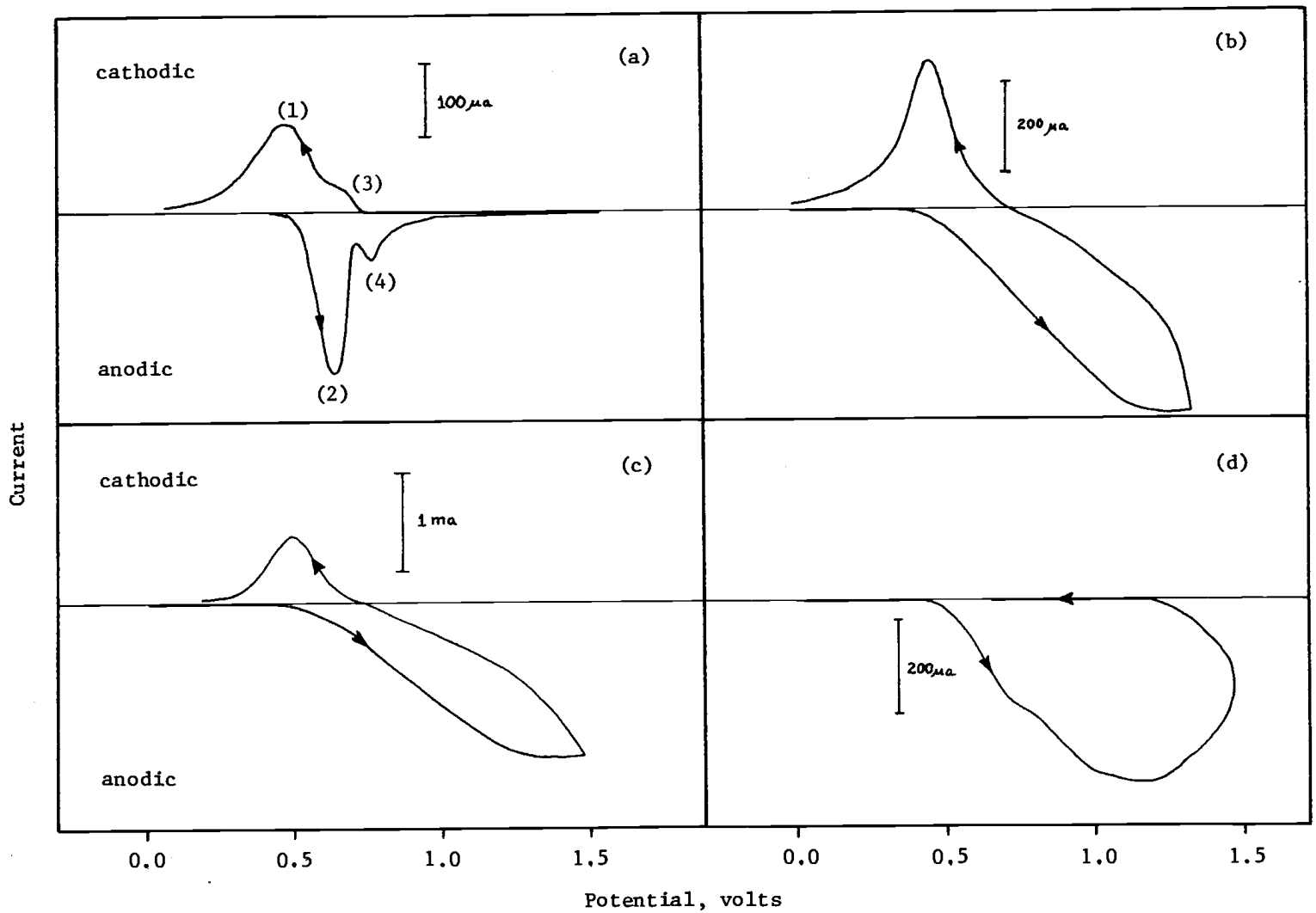

Figure 24. Effect of temperature on voltammetry curves obtained at a platinum electrode in triethylammonium dichlorocuprate(I); (a), 21°C; (b), 34°C; (c), 51°C; (d), 13°C.

voltages are variable depending on the age and history of the electrolyte.

The first reaction commenced at ca. 0.5 v with respect to the copper reference electrode. Following onset of the reaction a green deposit was observed adhering to the platinum working electrode. That the first anodic product is copper(II) is implied from the similarity between this potential and by the appearance of the product to those observed in the OTTLE coulmetric experiments.

Two anodic and cathodic peak combinations in Figure 24(a), (1) - (2) and (3) - (4), are related through redox reactions. These relationships were shown by anodic and cathodic cyclic scans of the voltage ranges between corresponding peaks. All four current peaks were observed at both platinum and glassy carbon electrodes.

The temperature dependence of peak shapes is shown in Figure 24. Polarograms at 34°C and 51°C, in addition to showing the expected increase in cell current, lack the definition observed at 21°C. The polarogram obtained at 13°C, made following the 51°C scan, shows the same lack of peak definition observed at 51°C. However, the loss of corresponding cathodic current peaks at 13°C indicates a change in state of the anodic deposit.

The appearance of unsymmetrical anodic current peaks, generally less than several hundred microamps, in the voltammograms of an electrolyte containing 5.9 M copper(I) is indicative of electrode passivation or blockage. In addition, a copper(II) chloride concentration of one molal was found to cause the fused salt mixture to become rigid after standing.

Similar current peaks and shapes observed in other systems (44, 46) have been attributed to electrode surface blockage. Mathematical modeling of a system where film formation on the electrode occurs and where current is controlled by the resistance of both solution and film predicts that both peak current and potential will depend on the square root of the scan rate (46). A plot of this function of scan rate versus peak current and potential at a platinum electrode in triethylammonium dichlorocuprate(I) is shown in Figure 25. Both relationships are linear for the electrolyte, in the range 2-100 mv/sec, in agreement with the relationship predicted for surface electrode blockage (46). This again indicates the overall effect to be brought about by a temperature-moderated formation of a copper(II) chloride film of high viscosity.

Polarization Studies

The cell used to study overpotential-current relationships is shown in Figure 26. Working and auxiliary electrode compartments were separated by a coarse glass frit. Efficient agitation of the electrolyte was accomplished with magnetic stirring.

Platinum working electrodes were pretreated by washing them with 8 M nitric acid and distilled water. The copper foil working electrode was lightly polished with No. 400 emery paper and washed with 4 M nitric acid followed by distilled water. In each experiment, the working electrode was insulated on one side with black Apiezon wax and positioned in the cell with the conducting face orthogonal to the direction of the auxiliary electrode. Working electrodes had geometric surface areas of 1 cm^2.

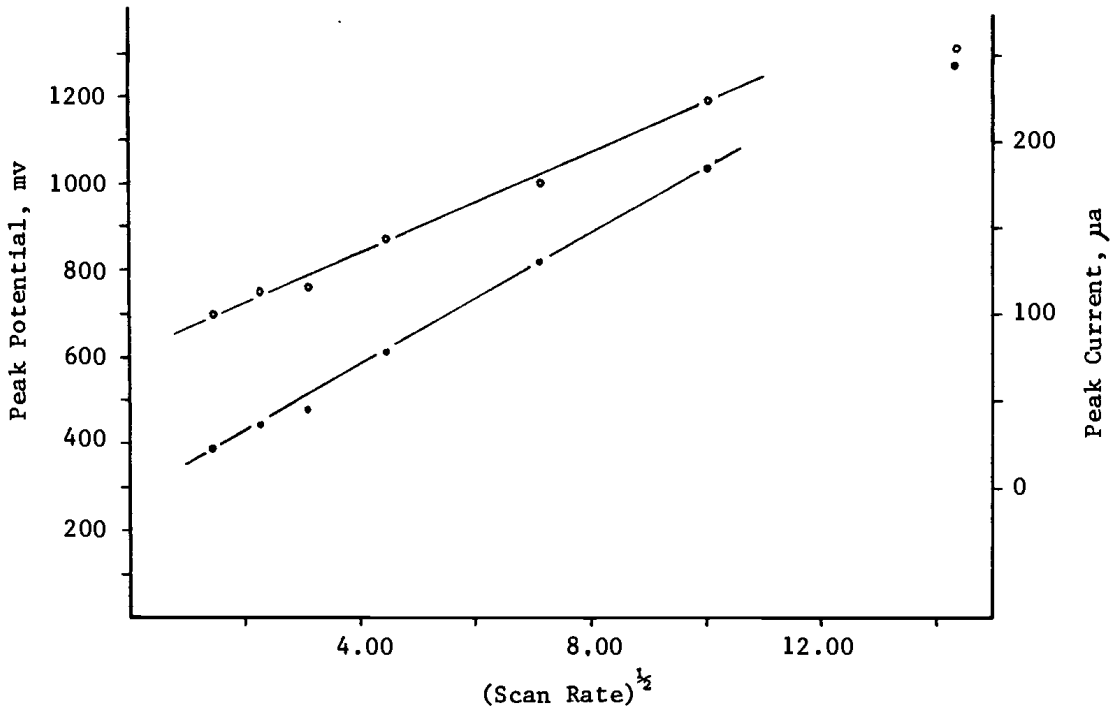

Figure 25. Plot of peak potential and current versus the square root of the potential scan rate; (o–o–o), peak potential; (•–•–•), peak current.

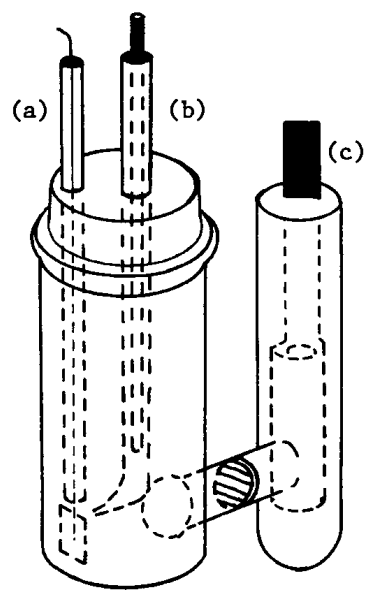

Figure 26. Cell used for overpotential measurements; (a), working, (b), reference and, (c), auxiliary electrodes.

The choice of reference electrode was dependent upon the working electrode metal. For overpotential measurements at a copper working electrode an 11 gauge copper wire was used as a reference electrode. Overpotential measurements at a platinum electrode in contact with a solution of copper(II) chloride in triethylammonium dichlorocuprate(I) were obtained using a spiral platinum wire reference electrode. An 18 cm^2 piece of copper foil was employed as an auxiliary electrode.

The effects of polarizing current on the potential adopted by a copper electrode in contact with stirred triethylammonium dichlorocuprate(I) are shown in Figures 27 and 28. Similar plots for copper in contact with a stirred fused salt mixture containing copper(I) chloride and triethylammonium chloride in a mole ratio of 1.2 to 1.0, respectively, are shown in Figures 29 and 30. Plots for a platinum electrode in contact with a stirred fused salt mixture containing copper(II) chloride are shown in Figures 31 and 32. Overpotential data above 20 mv in either direction were obtained galvanostatically and potentiostatically with no significant differences. Tafel regions in Figures 27, 29, and 31 are not obvious, although less curvature is observed at potentials above ± 300 mv. At these high potentials, however, other current limiting processes such as diffusion overpotential and ohmic polarization may become significant. Assuming that the charge transfer step is rate determining and that only one electron is involved in the electrochemical reactions of copper(I) and copper(II) chlorides, the well known approximations to the Butler-Volmer equation may be applied. For the overvoltage range $-120 \text{ mv} \geq \eta \geq 120 \text{ mv}$, the Butler-Volmer equation reduces to

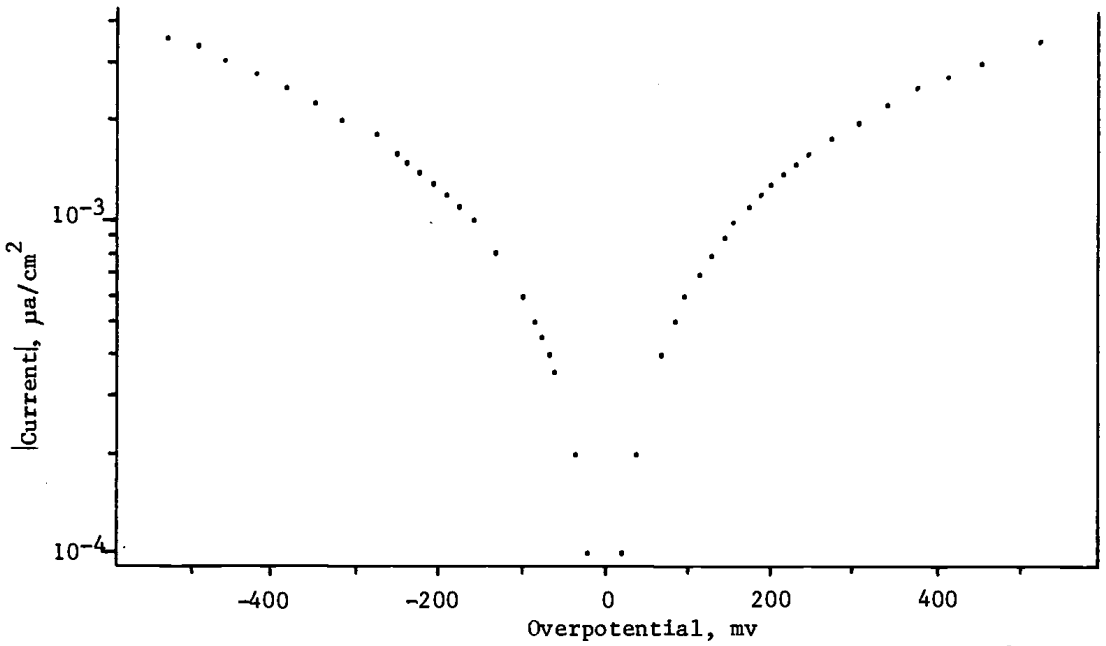

Figure 27. Plot of current density versus overpotential at a 1 cm^2 copper electrode in triethylammonium dichlorocuprate(I).

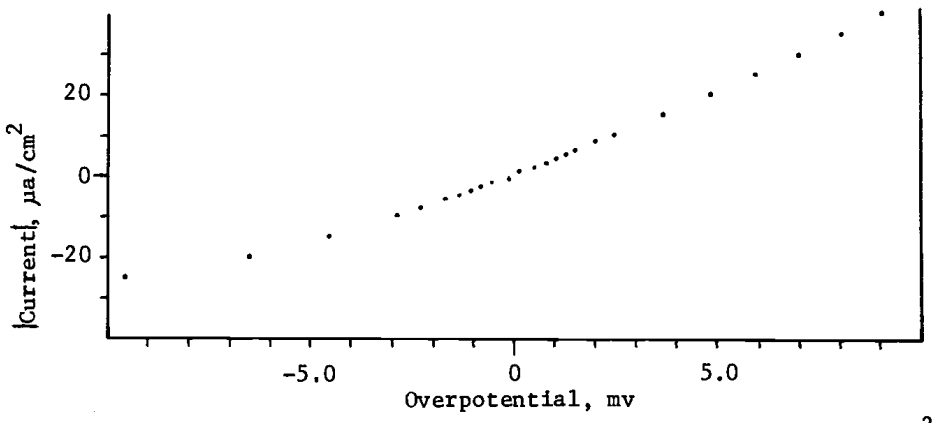

Figure 28. Plot of current density versus overpotential at a 1 cm^2 copper electrode in triethylammonium dichlorocuprate(I).

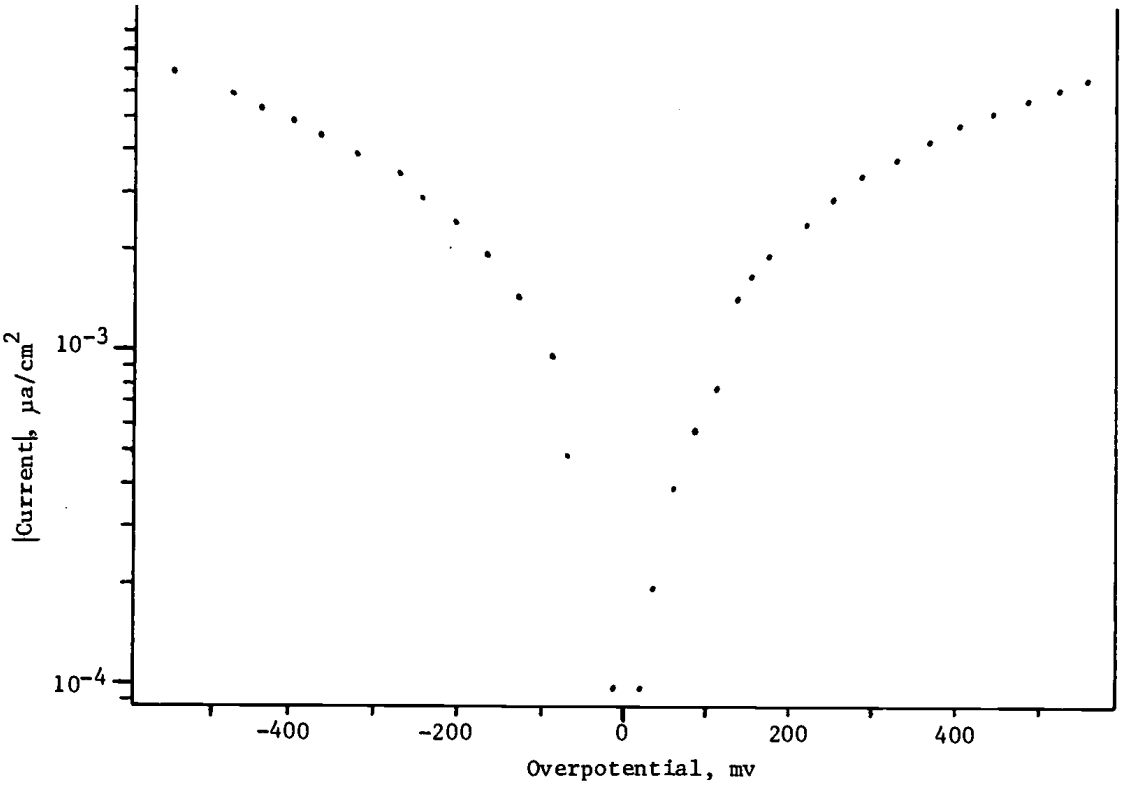

Figure 29. Plot of current density versus overpotential at 1 cm^2 Cu electrode in a fused salt solution of Et_3NHCl and CuCl in a mole ratio of 1 to 1.2.

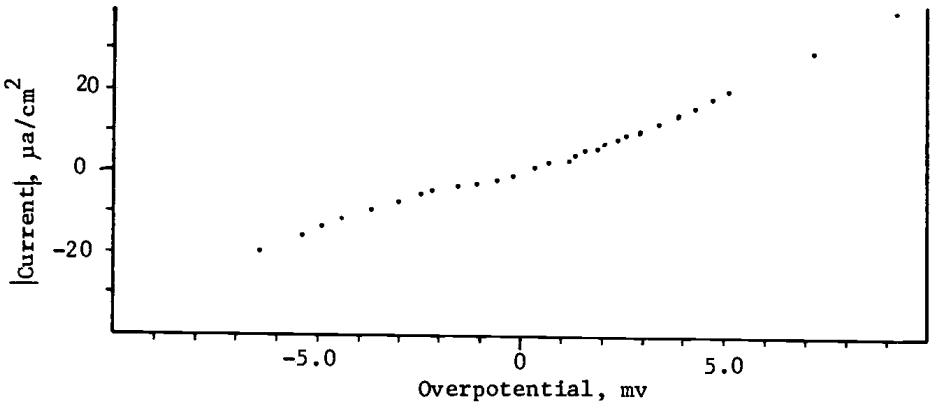

Figure 30. Plot of current density versus overpotential at a 1 cm^2 copper electrode in a fused salt solution of Et_3NHCl and CuCl in a mole ratio of 1 to 1.2.

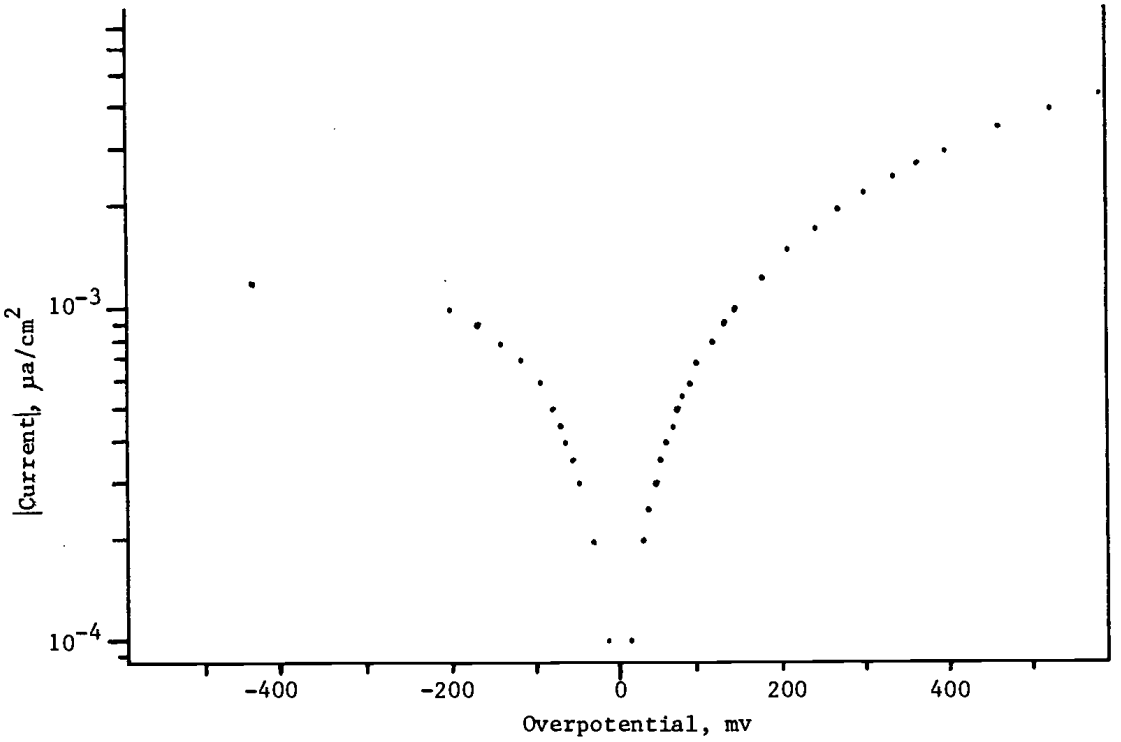

Figure 31. Plot of current density versus overpotential at a 1 cm^2 platinum electrode in a triethylammonium dichlorocuprate(I) solution containing 0.102 molal $CuCl_2$.

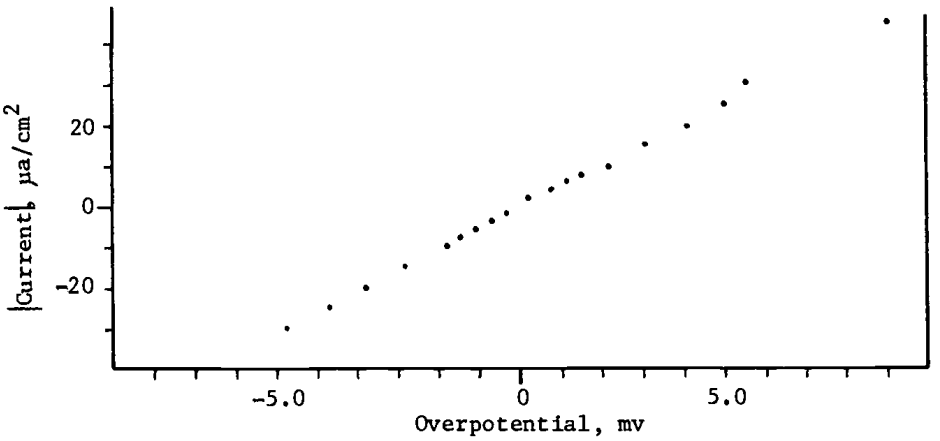

Figure 32. Plot of current density versus overpotential at a 1 cm^2 platinum electrode in a triethylammonium dichlorocuprate(I) solution containing 0.102 molal $CuCl_2$.

$$i_{anodic} = i_o e^{(1-\alpha)\eta F/RT} \quad \text{and} \quad i_{cathodic} = i_o e^{-\alpha\eta F/RT}$$

These high field approximations have been shown to be in error by +16.7%, +2.0%, and +1.0% for overvoltages of ± 50 mv, ± 100 mv, and ± 120 mv, respectively (41). Since Tafel slopes corresponding to the high field approximations were indistinct, the exchange current densities, i_o, were determined from data in the low overpotential regions, 10 mv ≥ η ≥ -10 mv. Under previously stated conditions the Butler-Volmer equation at low overpotentials reduces to

$$i = i_o \frac{F\eta}{RT}$$

Experimental Tafel slopes were constructed in Figures 27, 29, and 31 using exchange currents obtained in this manner. Lines were extrapolated from i_o to the current point yielding the highest slope for each of the polarization curves. Exchange current densities and transfer coefficients calculated from these slopes are shown in Table 4. For complex, multistep reaction mechanisms there is no requirement that $\alpha_{cathodic}$ be equal to $(1-\alpha_{anodic})$ (41). However, when the forward and reverse electrode reactions occur by the same mechanism, the sum of α_{anodic} and $\alpha_{cathodic}$ should be 1 (57, 58, 59). Transfer coefficients

Table 4. Transfer coefficients and exchange current densitites for $Cu/Et_3NHCuCl_2$ and $Pt/Et_3NHCuCl_2$ interfaces.

Interface	i_o (μa)	Anodic	Cathodic
$Cu/Et_3NHCuCl_2$	94	0.57	0.57
$Cu/Et_3NHCuCl_2$ + CuCl[a]	74	0.56	0.69
$Pt/Et_3NHCuCl_2$ + $CuCl_2$[b]	132	0.19	--

[a] 20 mole % excess CuCl

[b] 0.10 m $CuCl_2$

of 0.5 are generally expected when both branches of the polarization curve are symmetrical as in Figures 27 and 29. The asymmetry of Figure 31 probably indicates the presence of other overpotential phenomena, particularly severe in the case of the cathodic reaction.

Polarization data for 5 mv $\geq \eta \geq$ -5 mv shown in Figures 28, 30, and 32 indicate the electrode reactions to be reversible. The linear array of points on both sides of the rest potential shows the polarization resistance to be equal and relatively constant for anodic and cathodic processes. Although the reaction appears reversible with the use of slow measurement techniques, it is likely that methods requiring faster attainment of equilibrium would show the electrode systems to be quasi-reversible.

VI. PRELIMINARY STUDIES OF DESIGN AND PERFORMANCE OF ROOM TEMPERATURE FUSED SALT BATTERIES

Several types of fused salt batteries were prepared so as to assess various materials, electrolytes and cell geometries. The characteristics of various single cell battery configurations and electrolyte systems were evaluated with respect to current and voltage output trends. Some test batteries were prepared in an initially uncharged state, and then charged and tested. Discharge curves were obtained for several cells to provide estimates of effective energy storage capacities and current delivery rates. Although the batteries were capable of being recharged, no attempt was made to cycle them repeatedly or to obtain information on effects related to this type of operation.

A small cell used for measuring current and voltage outputs of batteries employing triethylammonium dichlorocuprate(I) or triethylammonium dichlorocuprate(I) - acetonitrile electrolytes is shown in Figure 33. Copper and Grafoil electrodes were used exclusively in this cell. Battery A-1 was prepared in a charged state and can be written as

$$Cu/Et_3NHCuCl_2{:}Et_3NHCl\ (1{:}1)/Et_3NHCuCl_2{:}CuCl_2\ (1{:}1.3)/Grafoil$$

Proportions of each component by weight are listed respectively in parentheses. The catholyte in this cell was prepared by mixing the fused salt and copper(II) chloride and adding the slurry to the battery. The copper(II) chloride in the cathode compartment was partially dissolved, so as to give a saturated solution, and partially present as a solid. The cell voltage and electrode areas are shown in Table 5 (page 79). A voltage-time curve for two discharge rates is shown in Figure 34. Output potentials were relatively constant at both rates of discharge,

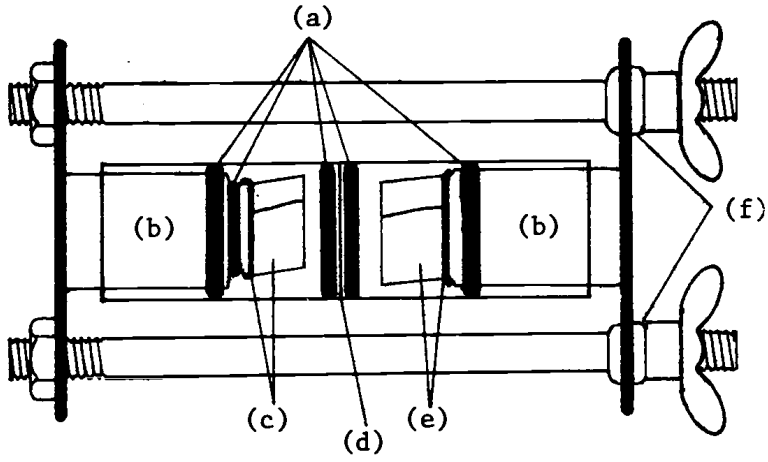

Figure 33. Type A battery; (a), O-ring seals and retainers; (b), Castaloy rods; (c), Grafoil cover and rolled Grafoil electrode;(d), paper spacer; (e), copper rod cover and rolled copper electrode; (f), rubber insulators.

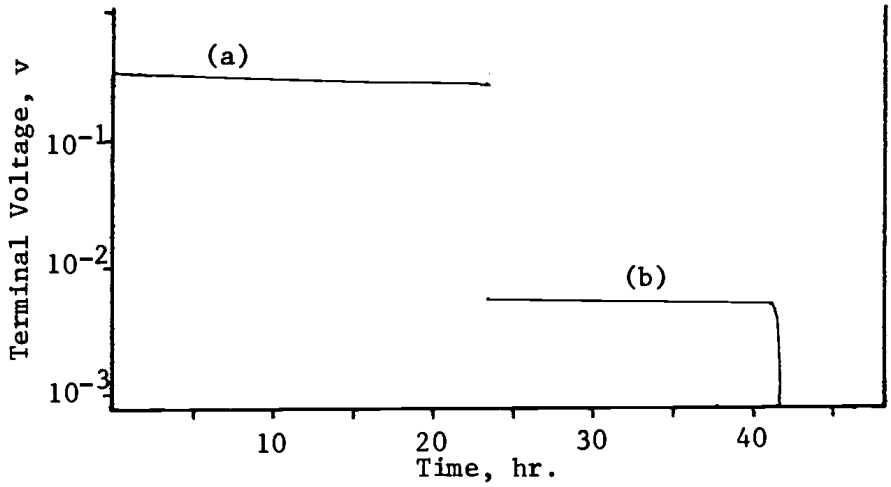

Figure 34. Discharge curve for battery A-1; (a), 1070 ohm load resistance; (b), 10 ohm resistance.

and up to cell death. The abrupt cessation of voltage resulted from internal short circuiting. Initially, the catholyte viscosity appeared similar to that of pure triethylammonium dichlorocuprate(I). However, upon examining the cell after discharge, the catholyte had become considerably more viscous. The viscosity of triethylammonium dichlorocuprate(I) is increased by the addition of copper(I) chloride or copper (II) chloride. An increase in the catholyte viscosity during battery discharge would therefore be expected to be partially due to dissolved copper(II) chloride and to the formation of copper(I) chloride since no excess triethylammonium chloride was present to form the lower viscosity triethylammonium dichlorocuprate(I) electrolyte.

Cell A-2, constructed using the identical cell casing described above but without rolled electrode elements was prepared with additional triethylammonium chloride in both anolyte and catholyte and can be written as

$Cu/Et_3NHCuCl_2:Et_3NHCl$ (1:0.58)$/Et_3NHCuCl_2:CuCl_2:Et_3NHCl$ (1:0.93:0.47)/Grafoil

The voltage output for this cell is listed in Table 5 and a discharge curve shown in Figure 38a (page 75). A rather low average output current of about 0.15 ma was monitored for 53 hours.

The open circuit voltages of cells A-1 and A-2 were about 0.75 v. The appearances of both cell discharge curves were also similar and indicate that considerable electrode polarization develops shortly after the cells begin operation. The magnitude of these polarization effects may be partially alleviated by lowering the electrolyte viscosity. Internal iR losses should also decrease with the viscosity.

A cell prepared using the arrangement of cell A-2 contained a 78:22 homogeneous mixture of triethylammonium dichlorocuprate(I) and acetonitrile as the solvent. The cell, A-3, can be written as

Cu/mixed solvent:Et_3NHCl (1.7:1)/mixed solvent:$CuCl_2$:Et_3NHCl (1.9:1:1)/Grafoil

The open circuit voltage of this cell is shown in Table 5. Discharge of the cell through a 2.0 ohm resistor resulted in an initial current of 1 ma which decreased over a 10-minute period to 0.1 ma. The effect of copper(II) chloride on the viscosity of the acetonitrile-triethylammonium dichlorocuprate(I) electrolyte was similar to that observed when copper(II) chloride was added to triethylammonium dichlorocuprate(I) (Section IV, Viscosities). Considerable thickening of the electrolyte did occur. The cell potential was about 0.03 v higher than in the two previous cells, presumably due to the modified solvent system.

Acetonitrile was employed as the sole solvent in cell A-4. The previous cell design, A-2, was again used. The cell was prepared in a charged state and can be written

Cu/Et_3NHCl:CH_3CN 1:1.5)/Et_3NHCl:CH_3CN:$CuCl_2$(1:2.5:1.9)/Grafoil

The open circuit voltage for this cell is listed in Table 5 and the discharge curve is shown in Figure 38b. As discharge proceeded the electrolyte viscosity increased as a consequence of triethylammonium dichlorocuprate(I) formation at both electrodes. Therefore, the battery internal resistance was expected to be at a minimum initially. The highest current output for this cell was 12 ma, during discharge through a 2.0 ohm resistor and represents a substantial improvement in

current output per unit electrode area over previous cells.

In order to increase the capacity of a battery prepared in an uncharged state, basically a rechargable cell, supplemental copper(I) chloride was added to the triethylammonium dichlorocuprate(I) anolyte and catholyte. This type of battery was prepared using a rolled electrode configuration. Batteries with rolled electrodes were generally prepared by sandwiching a sheet of Whatman chromatographic paper (No. 1 or 4) between flat anode and cathode sheets and rolling tightly. Depending on the system, electrolytes and reagents were added either before rolling or after insertion of the electrode assembly in the battery case. Unwrapped platinum or Grafoil cathodes were universally employed, but copper anodes were wrapped in Whatman chromatographic paper to inhibit dendritic growths and sloughing of electrolytic copper deposits. Graphite rods, held by friction, were used as leads to Grafoil electrodes and copper wire leads were soldered to anodes. Battery casings were made from short pieces of Pyrex tubing sealed at one end. Airtight seals were made with either Pyseal or Apiezon wax. This type of cell is shown in Figure 35. An example of such a cell prepared in the uncharged state, B-1, is described by

$$Cu/Et_3NHCuCl_2:CuCl\ (1:1)/Et_3NHCuCl_2:CuCl\ (1:1)/Grafoil$$

Before electrical measurements were obtained, a charging current of 22-27 ma was passed through the cell for 48 hours. This charge would give the cell a thoeretical capacity of 1.3 amp-hr. However, during charging an indeterminable fraction of the electrogenerated copper(II) chloride migrated to the cathode where it was reduced. This reaction, effectively being an internal short, made it impossible to determine

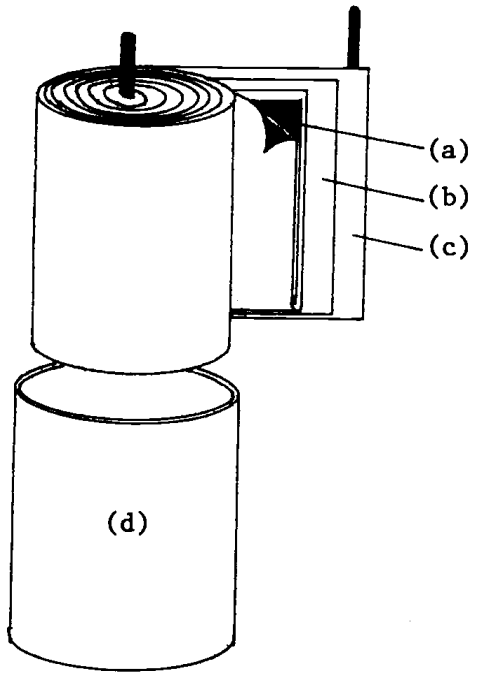

Figure 35. Rolled electrode battery; (a), copper foil anode wrapped in chromatographic paper; (b), paper spacer; (c), Grafoil electrode; (d), case.

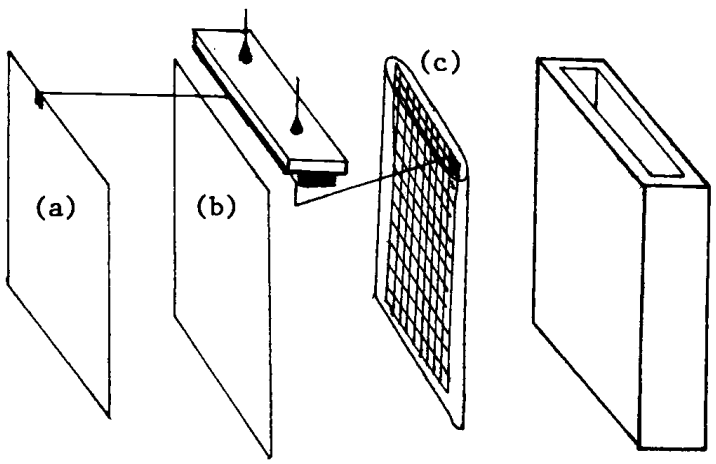

Figure 36. Plexiglas fused salt battery; (a), copper foil anode; (b), paper spacer; (c), platinum gauze cathode in separator bag.

the battery's true state of charge. The discharge curve is shown in Figure 38c and the output voltage in Table 5. Copper and Grafoil electrodes were separated by only 1-1.5 mm and this, in conjunction with the large electrode area, was responsible for the relatively high initial output current (37 ma). The terminal voltage remained fairly constant at 185 mv for about 10 minutes and then dropped sharply.

A battery similar to cell B-1 was prepared with triethylammonium dichlorocuprate(I) as the electrolyte-solvent. However, cell B-2 was prepared charged by applying pastes of triethylammonium chloride-triethylammonium dichlorocuprate(I) and copper(II) chloride-triethylammonium dichlorocuprate(I) to the copper foil and Grafoil electrodes respectively. Cell B-2 was

$$Cu/Et_3NHCl,Et_3NHCuCl_2/Et_3NHCuCl_2,CuCl_2/Grafoil$$

The discharge curve is shown in Figure 38d. The cell output voltage is listed in Table 5. The low discharge current reflects the high internal cell resistance brought about by dissolved copper(II) chloride. Cell current did, however, remain above 1 ma for over 10 hours.

Battery B-3 was prepared using rolled electrodes as in battery B-1, but with an acetonitrile solvent. Triethylammonium chloride and copper(II) chloride were applied directly to the copper foil and Grafoil electrodes, respectively, before rolling. After insertion of the electrode assembly, the case was filled with acetonitrile. The cell can be written as

$$Cu/Et_3NHCl,CH_3CN/CuCl_2,CH_3CN/Grafoil$$

The open circuit voltage of this cell gradually decreased, while

standing, from an initial 0.95 v to less than 0.80 v. This gradual decrease was a consequence of copper(II) chloride dissolving, penetrating the separator and diffusing to the copper anode. The cell discharge curve is shown in Figure 38e. Initial discharge current through the 2.0 ohm resistance was 220 ma, giving a starting power output of 0.097 watt. This represents the best current and operational voltage output obtained from any A or B cell. If a suitable separator were found which could prevent the diffusion of copper(II) chloride away from the cathode compartment, improvements in voltage and power output might be significant. The Whatman chromatographic paper separators certainly cannot effectively prevent mixing of the anolyte and catholyte. Copper(II) chloride dissolved in acetonitrile is known to oxidize copper metal (60) and this reaction is presumably responsible for the nearly complete self discharge of this cell in about one day.

The following two cell types, C and D, were used to test the ability of several separator materials to limit diffusion of copper(II) chloride from the cathode compartment to the anode.

C-type cells were prepared using a platinum gauze cathode and a copper anode as shown in Figure 36. The cell compartment was constructed from 0.125 inch Plexiglas. Preparation of the 6x5 cm copper foil anode consisted of lightly polishing it with No. 400 emery paper and washing it with distilled water. The cathode, a 6x6 cm piece of platinum gauze, was coated with an aqueous slurry of copper(II) chloride and Methocel. The slurry was prepared by grinding two grams of copper(II) chloride dihydrate with 1 ml of a 1% aqueous solution of Methocel 60 HG. After the slurry had been applied the electrode was

heated at 110°C until the copper(II) chloride had become dehydrated. Prior to each experiment, the platinum gauze was cleaned with 8 M nitric acid and distilled water. Separators in the form of envelopes were prepared from sheet cellophane, dialysis tubing and Amerlite WB-2 (weakly basic) anion exchange paper. Envelopes were prepared by cutting separator material to the desired size and sealing the edges with a low melting tar.

Battery C-1 was prepared in a charged state using sheet cellophane as a separator and can be written as

$$Cu/Et_3NHCuCl_2/Et_3NHCuCl_2,CuCl_2/Pt$$

The platinum gauze cathode was coated with copper(II) chloride dimensionally stabilized with a methylcellulose binder already described. The open circuit voltage of this cell is listed in Table 5. The voltage was lower than observed in earlier cells and could possibly be an effect of the binder. An output current of only 2.5 μa was obtained when the cell was discharged through 1700 ohms as a result of the large separator resistance.

Investigations of low viscosity fused salt-acetonitrile electrolytes were carried out in the battery shown in Figure 37. The cell casing was constructed from 0.25 inch PVC sheeting. An airtight assembly was obtained by bolting the cell wall and the rubber gasket to the main body. Electrical lead openings were sealed with a low melting tar.

This cell deisgn used three 4.5x4.5 cm copper anodes and three 4.5x4 cm Grafoil cathodes. Identical electrodes were internally connected to each other and to external leads with springs. Copper electrodes were pretreated with dilute nitric acid, polished with No. 400

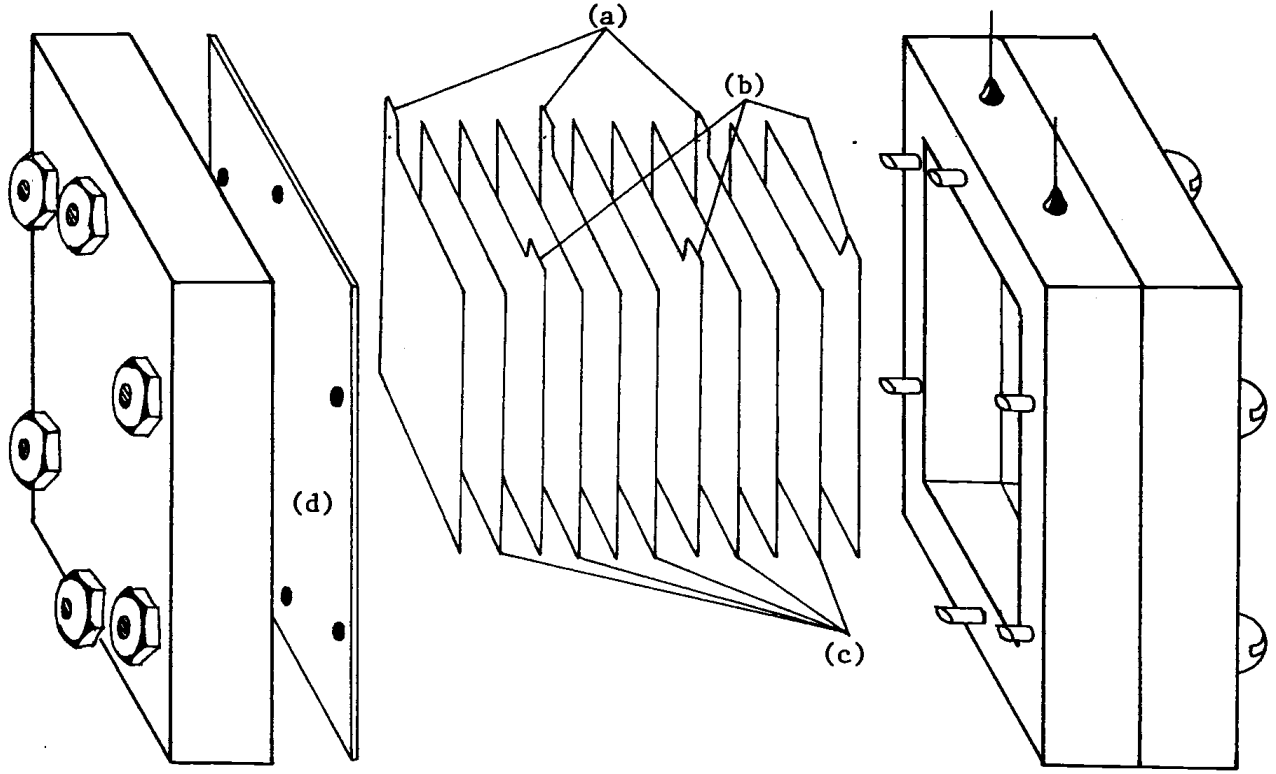

Figure 37. PVC fused salt battery; (a), copper foil anodes; (b), Grafoil electrodes in separator bags; (c), paper spacers; (d), rubber gasket.

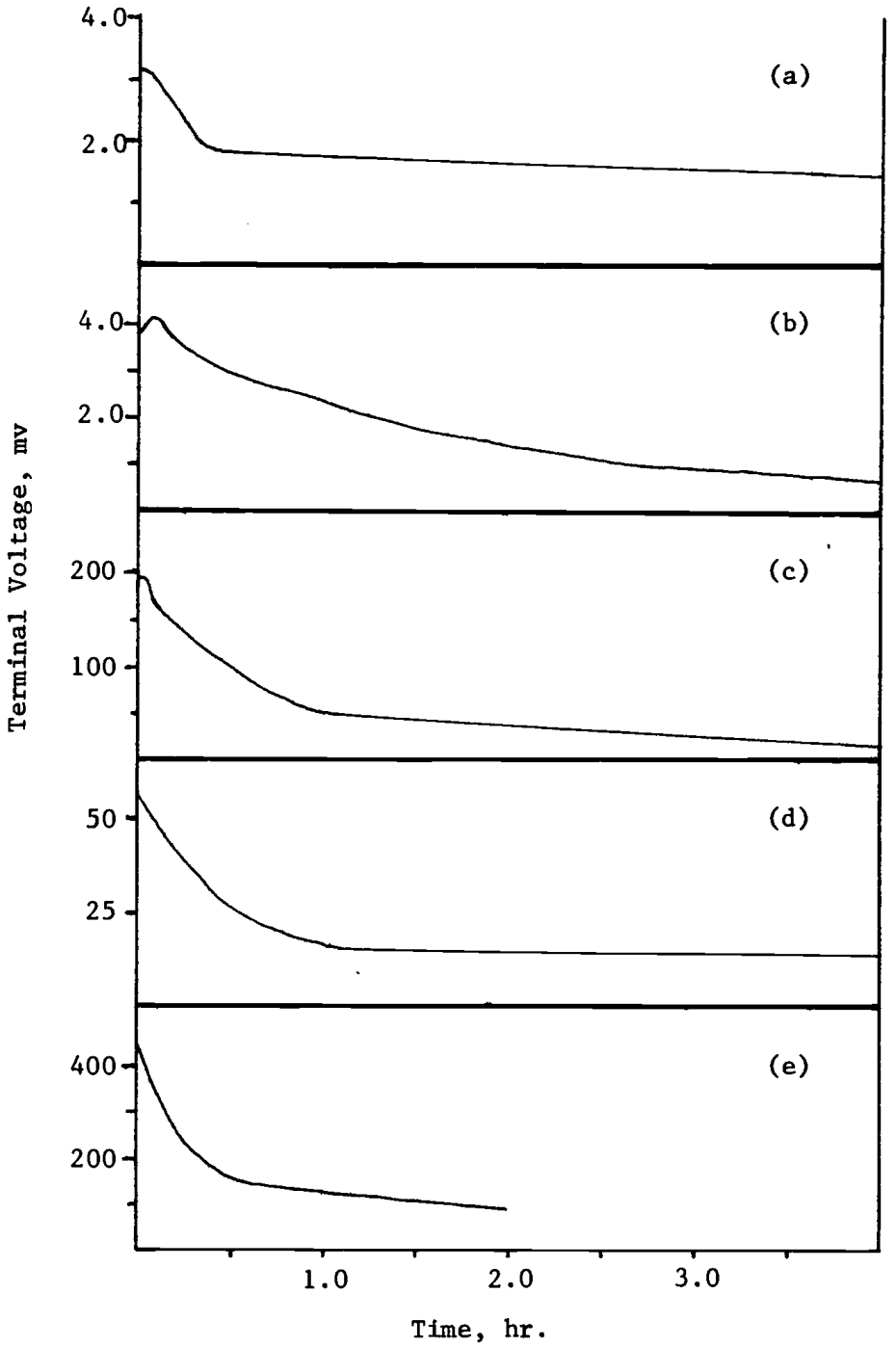

Figure 38. Discharge curves for A and B type batteries; (a), discharge of cell A-2 through 10.5 ohms; (b), discharge of cell A-4 through 4.9 ohms; (c), discharge of cell B-1 through 4.9 ohms; (d), discharge of cell B-2 through 9.9 ohms; (e),discharge of cell B-3 through 2.0 ohms.

emery paper and washed with distilled water. Grafoil electrodes were not pretreated and had to be discarded after use. Separators made from sheet cellophane, dialysis tubing and Amberlite WB-2 anion exchange paper were prepared in the same manner as described for the Plexiglas cell above. Components of the cell were arranged in the following sequence: copper foil, Whatman chromatographic paper spacer, separator envelope containing a Grafoil cathode.

Cell D-1 can be written

$Cu/Et_3NHCuCl_2, CH_3CN/Et_3NHCuCl_2, CH_3CN/Grafoil$

The electrolyte was 25%, by volume, acetonitrile in triethylammonium dichlorocuprate(I). Before making any electrical measurements a charging current of 10 ma was maintained for one hour. The operating voltage is listed in Table 5. The high resistance of sheet cellophane separators reduced the discharge current, through a 18 ohm resistance to only about 1 ma.

Another cell, C-2, was prepared in the same manner as C-1 except dialysis tubing was substituted for sheet cellophane as the separator material. The output voltage for this battery is shown in Table 5. The discharge current was again quite low because of high separator resistance.

Battery D-2 was also prepared identically to D-1, but with dialysis tubing replacing sheet cellophane as the separator material. The open circuit voltage for this cell is listed in Table 5. The cell was charged for 30 minutes before any measurements were made. A potential of 7.5 volts was required to pass a 10 ma current through the cell, indicating the presence of a substantial internal resistance.

Substitution of the cellophane separator in cell C-1 with anion exchange paper (chloride form) was attempted in cell C-3. The open circuit voltage for this cell is listed in Table 5. Copper(II) chloride was observed penetrating the separator material so self discharge was occurring. The voltage-time discharge curve is shown in Figure 39a.

The behavior of an acetonitrile-triethylammonium dichlorocuprate(I) electrolyte system used in conjunction with anion exchange separators was investigated with battery D-3. The cell and electrolyte were the same as described in cell D-1. The open circuit voltage is listed in Table 5. The cell, prepared uncharged, required an initial charging potential of only 0.75 v to maintain a 100 ma current. The charging was continued for two hours. The discharge curve is shown in Figure 39b. Self discharge of this cell was nearly complete in about one day.

The highest open circuit voltage produced by a single cell of the type $Cu/Et_3NHCuCl_2, Et_3NHCl/Et_3NHCuCl_2, Et_3NHCl, CuCl_2/Grafoil$, where Et_3NHCl and $CuCl_2$ were each present partially in the solid phase and partially dissolved, was 0.75 v. Modifying the electrolyte by addition of acetonitrile can increase the cell voltage to at least 0.95 v, but an efficient separator is necessary to prevent internal chemical short circuiting. Discharge curves obtained from all batteries show that cell potentials fell rapidly after discharge began. This most likely results from slow diffusion of electroactive species in the vicinity of the anode and cathode. The highest initial discharge currents were obtained for batteries which had acetonitrile added to the electrolyte: B-3, 220 ma through 2.0 ohms; D-3, 69 ma through 9.0 ohms. However, none of the fused salt batteries could sustain maximum output currents

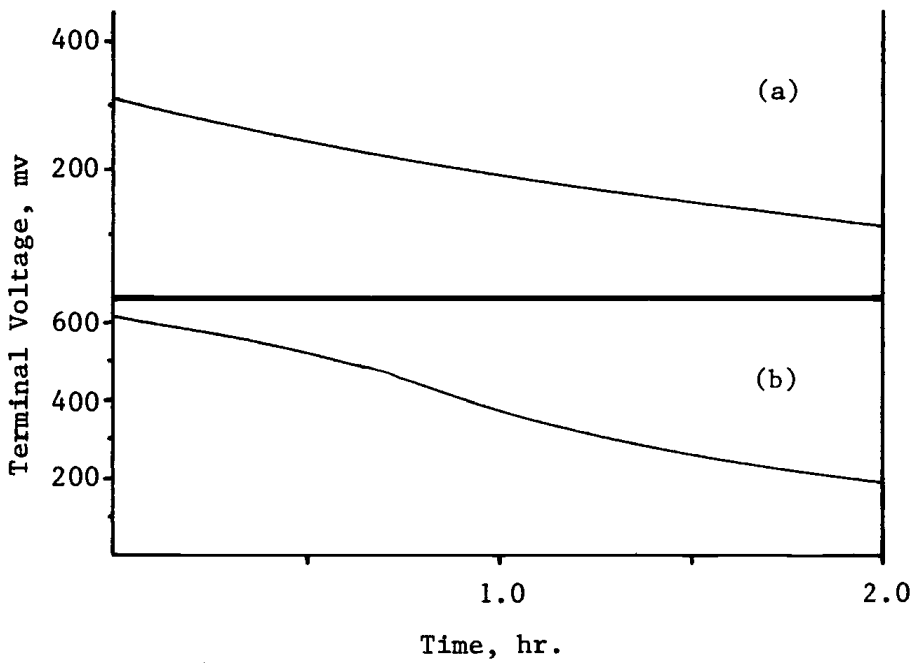

Figure 39. Discharge curves for C and D type cells; (a), discharge of cell C-3 through 9.0 ohms; (b), discharge of cell D-3 through 9.0 ohms.

and potentials for more than a few minutes, and this certainly would limit the application of C or D size fused salt cells of this design to systems which would impose only a very low current draw on individual cells.

Table 5. Electrode and output data for fused salt batteries.

Cell	Open Circuit Voltage volts	Anode Area[a] cm^2	Cathode Area[a] cm^2
A-1	0.747	10	10
A-2	0.746	23	24
A-3	0.78	1.1	1.1
A-4	--	1.1	1.1
B-1	0.540	252	252
B-2	0.68	120	120
B-3	0.95 (variable)	120	120
C-1	0.58	60	6x6 Pt gauze
C-2	0.56	60	6x6 Pt gauze
C-3	0.61	60	6x6 Pt gauze
D-1	0.80	122	108
D-2	0.72	122	108
D-3	0.68	122	108

[a] total surface area exposed to electrolyte

VII. SUGGESTIONS FOR FURTHER BATTERY RESEARCH

The performance of room temperature fused salt batteries prepared here can be described as poor in comparison with similarly sized conventional dry cell batteries. Since a simple scale-up of these fused salt cells would be of little value from the standpoint of cell power density, further improvements in cell performance should evolve from design considerations and an understanding of what factors are important in electrode polarization and influence the electrolyte resistance.

General trends in the performance of fused salt batteries based on triethylammonium dichlorocuprate(I) can be partially understood from the effect of the solutes, copper(I) chloride and copper(II) chloride, on the electrolyte conductivity. Both of these salts increase the viscosity and lower the conductance of the liquid. The internal resistance of these cells certainly results in significant iR losses and the increased viscosity probably raises the minimum temperature at which the cell could operate. Thus, for operating conditions at or below room temperature, the use of a resistance and viscosity reducing additive would be of considerable value.

Lowering the electrolyte viscosity by addition of acetonitrile could improve battery performance if an efficient separator were used. An anionic ion-exchange membrane, Amfion A-60, has been shown to work effectively with the acetonitrile - copper(I) - copper(II) system (61). In addition, the use of solid additives should also be considered for the same reasons. Lithium chloride and triethylammonium chloride are only sparingly soluble and have been found to decrease the electrolyte conductivity, but perhaps some other salts might be used to advantage.

The effect of electrode polarization during charge or discharge in batteries increases the inefficiency associated with the transfer of electrical energy. The overpotential-current relationships observed with the triethylammonium chloride - copper(I) chloride - copper(II) chloride electrolyte systems indicate that electrode current densities of $\pm 10^{-3} A/cm^2$ may only be attained when the electrode has been polarized approximately ± 100 mv. In view of the relatively low single cell potential for this battery, 0.75 v, the decrease in cell potential during current draws of ca $10^{-3} A/cm^2$ would result in substantial power losses within the cell. The most straightforward way of compensating for the low exchange current density, ca $10^{-4} A/cm^2$, would be to employ electrodes of very high surface to volume ratio. Porous electrodes of Reticulated Vitreous Carbon, with surface areas in the range of 66 cm^2/cm^3, could increase operating currents and voltages for batteries of comparable size to those already studied, thereby increasing their power output.

Polarization effects brought about by anodic film formation and electrode blockage, during battery charging, could be circumvented by using sufficiently low charging rates or addition of a low viscosity solvent such as acetonitrile to the electrolyte. A decrease in viscosity would facilitate the diffusion of nacent copper(II) away from the anode before a semi-fluid film develops. The use of large surface area anodes, mentioned earlier, would also decrease the importance of this effect.

BIBLIOGRAPHY

1. J. T. Yoke, J. F. Weiss and G. Tollin, Inorg. Chem., 2, 1210 (1963).

2. D. D. Axtell, B. W. Good, W. W. Porterfield and J. T. Yoke, J. Am. Chem. Soc., 95, 4555 (1973).

3. W. W. Porterfield and J. T. Yoke, A.C.S. Adv. Chem. Ser. 150, 104 (1976).

4. J. H. R. Clarke and G. J. Hills, Chem. in Britian, 9, 12 (1973).

5. J. E. Gordon, in Techniques and Methods of Organic and Organometallic Chemistry, Vol. I, D. B. Denny, Ed., M. Dekker, New York, 1969, p. 51.

6. F. M. Hurley and T. P. Wier, J. Electrochem. Soc., 98, 203 (1951).

7. G. W. Parshall, J. Am. Chem. Soc., 94, 8716 (1972).

8. W. T. Ford, R. J. Hauri and D. J. Hart, J. Org. Chem., 38, 3916 (1973).

9. H. Remy and G. Laves, Chem. Ber., 66 571 (1933).

10. J. R. Clifton and J. T. Yoke, Inorg. Chem., 5, 1630 (1966).

11. J. R. Clifton and J. T. Yoke, Inorg. Chem., 6, 1258 (1967).

12. T. G. Sukhova, O. N. Temkin and R. M. Flid, Russ. J. Inorg. Chem., 14, 483 (1969).

13. T. G. Sukhova, O. N. Temkin and R. M. Flid, Russ. J. Inorg. Chem., 15, 949 (1970).

14. A. F. Wells, Structural Inorganic Chemistry, Third Ed., Oxford University Press, London, 1962.

15. J. R. Clifton, Dissertation, Oregon State University, 1966.

16. W. E. Hatfield and T. S. Piper, Inorg. Chem., 3, 841 (1964).

17. G. C. Allen and N. S. Hush, Prog. Inorg. Chem., 8, 357 (1967).

18. N. S. Hush, Prog. Inorg. Chem., 8, 391 (1967).

19. H. McConnell and N. Davidson, J. Am Chem. Soc., 72, 3168 (1950).

20. M. Mori and S. Fujiwara, Bull. Chem. Soc. Japan, 36, 1636 (1963).

21. D. Culpin et al., Chem. Commun., 450 (1965).

22. J. O'M. Bockris, in Modern Aspects of Electrochemistry, No. 2, Academic Press, New York, 1959, p. 168.

23. J. O'M. Bockris, J. A. Kitchener, S. Ignatowicz and J. Tomlinson, Trans. Farad. Soc., 48, 75 (1952).

24. H. Bloom and E. Heymann, Proc. Roy. Soc. (Lon.), 188 A, 392 (1947).

25. G. J. Janz, C. Solomons and H. J. Gardner, Chem. Rev., 58, 461 (1958).

26. G. Kortum, Treatise on Electrochemistry, Second Ed., Elsevier, New York, 1965, Chap. 7.

27. J. O'M Bockris and A. K. N. Reddy, in Modern Electrochemistry, Vol. I, Plenum Press, New York, 1972, Chap. 6.

28. K. Krishnamoorthy and S. Omayorupakam Pillai, Indian J. Phys., 49, 155 (1975).

29. C. V. Suryanarayana and V. K. Venkatesan, Acta. Chem. Acad. Sci. Hung., 16, 451 (1958).

30. H. Bloom, B. Harrap and E. Heymann, Proc. Roy. Soc., 194 A, 237 (1948).

31. I. Delimarski and B. F. Markov, Electrochemistry of Fused Salts, Sigma Press, 1961, Chap. 1.

32. J. Frenkel, Kinetic Theory of Liquids, Oxford Univ. Press, London, 1947, p. 441.

33. I. Yaffee and E. Van Artsdalen, J. Phys. Chem., 60, 1125 (1956).

34. J. J. Lingane, Electroanalytical Chemistry, Interscience, New York, 1958, p. 40.

35. J. O'M. Bockris and B. E. Conway, Modern Aspects of Electrochemistry, No. 1, Butterworths, London, 1954, p. 192.

36. J. Koryta, J. Dvorak and V. Bohackova, Electrochemistry, Methueu and Co., 1973, p. 165.

37. L. P. Hammett and A. E. Lorch, J. Am. Chem. Soc., 55, 70 (1933).

38. R. H. Cousens, D. J. G. Ives and R. W. Pittman, J. Chem. Soc., 3972 (1953).

39. D. C. Hamby and A. B. Scott, J. Electrochem. Soc., 115, 704 (1968).

40. J. O'M. Bockris and Z. Nagy, J. Chem. Ed., 50, 839 (1973).

41. J. O'M. Bockris and A. K. N. Reddy, Modern Electrochemistry, Vol. 2, Plenum Press, New York, 1972, Chaps. 8, 9.

42. J. Koryta, J. Dvorak and V. Bohackova, Electrochemistry, Methuen and Co., 1973, Chap. 4.

43. G. Kortum, Treatise on Electrochemistry, Second Ed., Elsevier, New York, 1965, Chap. 12.

44. T. Erdey-Gruz, Kinetics of Electrode Processes, Adam Hilger, London, 1972, Chap. 7.

45. J. O'M. Bockris, Modern Aspects of Electrochemistry, No. 2, Academic Press, New York, 1959, pp. 262-342.

46. A. J. Calandra, N. R. DeTacconi, R. Pereiro and A. J. Arvia, Electrochimica Acta, 19, 901 (1974).

47. W. J. Muller, Trans, Farad. Soc., 27, 737 (1931).

48. D. R. Rosseinsky and R. E. Malpas, Nature, 258, 314 (1975).

49. E. Yeager and E. Schwartz, in The Primary Battery, Vol. I, G. Heise and N. Cahoon, Ed., Wiley and Sons, New York, 1971, Chap. 2.

50. J. O'M. Bockris and A. K. N. Reddy, Modern Electrochemistry, Vol. 2, Plenum Press, New York, 1972, Chap. 11.

51. R. N. Keller and H. D. Wycoff, Inorg. Syn., 2, 1 (1946).

52. T. DeAngelis and W. Heineman, J. Chem. Ed., 53, 594 (1976).

53. I. B. Joedicke, Dissertation, Oregon State University, 1976.

54. M. Sheely, Ind. Eng. Chem., 24, 1060 (1932).

55. J. B. Segur, in Glycerol, C. Miner and N. Dalton, Eds., Reinhold, New York, 1953, pp. 278-281.

56. W. J. Ingram, J. Assoc. Official Anal. Chem., 50, 397 (1967).

57. P. van Rysselberghe, Electrochim. Acta., 8, 583, 709 (1963).

58. P. van Rysselberghe, Electrochim. Acta., 9, 1547 (1964).

59. P. van Rysselberghe, Electrochim. Acta., 10, 107 (1965).

60. H. H. Morgan, J. Chem. Soc., 123, 2901 (1923).

61. B. Kratochvil and K. R. Betty, J. Electrochem. Soc., 121, 851 (1974).